UNIVERSITY OF ZIMBABWE

FACULTY OF ENGINEERING

DEPARTMENT OF CIVIL ENGINEERING

IMPACT OF LAND USE CHANGE AND INCREASED AGRICULTURAL WATER USE ON THE INCOMATI RIVER FLOW REGIME

EURICO BRAZ CARLOS MACUÁCUA

MSc. THESIS IN IWRM

HARARE, JUNE 2011

UNIVERSITY OF ZIMBABWE

FACULTY OF ENGINEERING

DEPARTMENT OF CIVIL ENGINEERING

In collaboration with

IMPACT OF LAND USE CHANGE AND INCREASED AGRICULTURAL WATER USE ON THE INCOMATI RIVER FLOW REGIME

By

EURICO BRAZ CARLOS MACUÁCUA

Supervisors

DR. M. J. TUMBARE
DR. D. JUIZO
MR. A. MHIZHA

A thesis submitted in partial fulfillment of the requirements for the degree of Master of Science in Integrated Water Resources Management of the University of Zimbabwe

June 2011

DECLARATION

I, **Eurico Braz Carlos Macuácua**, declare that this research report is my own work. It is being submitted for the degree of Master of Science in Integrated Water Resources Management (IWRM) at the University of Zimbabwe. It has not been submitted before for any degree of examination in any other University.

Date: ____________________

Signature: _____________________

The findings, interpretations and conclusions expressed in this study do neither reflect the views of the University of Zimbabwe, Department of Civil Engineering nor of the individual members of the MSc. Examination Committee, nor of their respective employers.

TABLE OF CONTENTS

LIST OF TABLES

LIST OF FIGURES

LIST OF EQUATIONS

LIST OF ABBREVIATIONS

ARA-Sul	South Regional Water Administration
AVHRR	Advanced Very High Resolution Radiometer
CENACARTA	National Centre for Remote Sensing and Cartography
DEM	Digital Elevation Model
DSMW	Digital Soil Map of the World
DWA	Department of Water Affairs
FAO	(United Nations) Food and Agriculture Organization
FDC	Flow Duration Curve
GBHM	Geomorphologically Based Hydrological model
GeoSFM	Geospatial Stream Flow Model
GIS	Geographical Information Systems
GLCC	Global Land Cover Characterization
ICMA	Incomati Catchment Management Agency
IIMA	Interim IncoMaputo Agreement
ILWIS	Integrated Land and Water Information System
ITC	International Institute for Geo-Information Science and Earth Observation
IWAAS	Inkomati Water Availability Assessment Study
IWRM	Integrated Water Resource Management
JIBS	Joint Incomati Basin Study
NOAA	United States National Oceanic and Atmospheric Administration
PET	Potential Evapotranspiration
PRIMA	Progressive Realisation of the IncoMaputo Agreement
RCN	Runoff Curve Number
RFE	Rainfall Estimates
SCS	Soil Conservation Service
TIA	Tripartite Interim Agreement
TPTC	Tripartite Permanent Technical Committee
USGS	United States of Geological Survey
WAFLEX	Water Allocation Flow model in Excel

DEDICATION

To my parents Mr. Carlos Macuácua and Mrs Isáura Facela
To my brother and sisters for the encouragement and moral support
To Jorfélia Chilaule for the encouragement

ACKNOWLEDGEMENTS

Thanks to the Almighty for keeping me all the way throughout the study. I also want to acknowledge and thank the following people for the contributions they made towards this project:

My sincere gratitude goes to my supervisors Dr M. J. Tumbare, Dr D. Juizo and Mr. A. Mhizha, for their diligent guidance, valuable suggestions and careful reading and correction of this thesis.

South Regional Water Administration (ARA-Sul) for allowing me to join the Waternet Regional Masters Programme. My special gratitude goes to the General Director Eng. Olinda Sousa, Mr. Agostinho Vilanculos, Eng. Jaime Mianga, Dr. Humberto Gueze, to mention a few.

My special tribute goes to Eng. Ivo Van Haren for providing me with valuable data and information and for facilitating valuable meetings with other international experts for assistance and support.

Dr. T. Sawunyama for the valuable databases and reports.

My special tribute goes to Yaone Monyamane for being always available and especially by helping me improving my English.

Waternet for sponsoring me to attend the Masters Programme, I believe the knowledge I have acquired throughout the eighteen months will make a difference in my personal and other people's lives. My special thanks to the staff members of the Department of Civil Engineering of the University of Zimbabwe.

Lastly, but certainly, not least, my family, friends, workmates, classmates, for their moral support throughout my studies and to those that I can not mention by name, thanks a lot and may God bless you all.

ABSTRACT

The Incomati River basin has been experiencing a decrease in river flows since the 1970's. At the same time its catchment area has undergone severe land use changes and increased water abstractions. Further water abstractions are planned for the future and this will pose a threat to downstream users including the river's estuary ecosystem. Studies that investigate the effect of different natural and human induced factors to the downstream flow regime are lacking in the basin. Thus, the objective of this study was to assess the effect of land use changes and increased agricultural water abstractions on the lower Incomati River flow regime. The outputs from the study could be useful as relevant information in the negotiation of reallocation of water among the countries sharing the basin as well as in recommending appropriate IWRM practices to minimize the foreseen negative impacts.

Spearman Rank Correlation Test was used to examine the historical trend in streamflows and agricultural water abstractions. The Geospatial Stream Flow Model (GeoSFM) was integrated with remote sensing and GIS to model the impact of land use changes on river flow regime. Spearman Rank Correlation Coefficients of *Rsp=-0.57 and Rsp=1* confirmed changes on streamflows and in agricultural water abstraction at the border gauge station of Ressano Garcia (E-23) with significance levels of 99.9% and 99% respectively. Land use maps of 1990, 2000, 2004 and 2010 derived from classification of Landsat TM images were fed into the GeoSFM and the results showed occurrence of significant changes ($p<0.05$) in streamflows in the sub-basins 26 and 33. These changes were more in terms of peak flows, time to peak and the response to rainfall events. The 2010 land use scenario produced hydrographs which responded faster to rainfall events than the 1990 land use. The peak flows generated by the 2010 land use hydrograph were of higher magnitude and steep rise to peak than those of 1990. These results suggest that the reduction in streamflows at the border station of Ressano Garcia can be attributed to other factors other than land use changes. Thus, IWRM strategies focusing on land use optimisation are recommended for further investigation and implementation in the affected sub-basins.

Key words: *Agricultural water abstractions, GeoSFM, hydrograph, Incomati, land use changes, streamflows*.

CHAPTER 1

1.0 INTRODUCTION

The Incomati River basin is situated in the south-eastern part of the African continent and is shared by South Africa, Swaziland, and Mozambique. The basin is relatively small (47,600 km^2) compared to many other basins in Africa such as Congo (3,670,000 km^2), Zambezi (1,359,000 km^2) and Orange/Senqu (848,000 km^2), but it is of strategic importance as it is located in an area of intense development, which results in a considerably high demand of its water resources. The level of water abstraction in the Incomati River is very high and the actual water demand is projected to increase in the future as a result of further economic development and population growth (Nkomo and van der Zaag, 2004; LeMarie *et al.*, 2006). Consumptive use of surface water amounts to more than 1,880 million cubic metres per annum (Mm^3/a), which represents 51% of the average amount of surface water generated in the basin (Vaz and van der Zaag, 2003). The major water consumers, accounting for 91% of all consumptive water uses, are the irrigation and forest plantation sectors, followed by inter-basin water transfers to Umbeluzi basin and Olifants catchment in the Limpopo basin (Vaz and van der Zaag, 2003).

The high level of water commitment in the Incomati basin since the 1970's showed the need for cooperation among the three countries sharing the basin. In this context, many Agreements have been reached among the three countries and of significance is the Tripartite Interim Agreement (also called IncoMaputo Agreement) of 2002. This Agreement is aimed at promoting cooperation among the three countries to ensure the protection and sustainable utilization of the water resources of the Incomati and Maputo watercourses (TIA, 2002). The Agreement was intended to cover a period of time until comprehensive water agreements can be reached for both basins. Although the agreement acknowledged the already visible high water commitment level of the Incomati basin, it made allowance for further developments taking into consideration their importance in each of the countries. Thus, with full development as allowed by the Agreement, total abstractions in the basin will increase to more than 2,340 Mm^3/a and this will result in a severe decrease of river flow downstream in Mozambique and will impact negatively in estuary ecosystems (van der Zaag, 2008).

However, Article 10 of the Tripartite Interim Agreement provides a platform for reallocation of water among the parties after thorough studies that recommended such practices of water use and allocation have been conducted. Thus, this study aims at assessing the effect of land use change and increased agricultural water demand on the river flow regime in order to generate knowledge and information which could be useful in the negotiation of reallocation of water among the three countries sharing the basin. This is done through the Tripartite Permanent Technical Committee (TPTC) which is the body responsible for the operational implementation of the Agreement. Furthermore, the study will also culminate in generation of recommended practices in line with IWRM to minimize the negative impact of land use change and increased water abstractions in the river flow regime in Mozambique.

1.1 Problem Statement

The lower Incomati River basin has experienced changes in flow regimes due to many factors. The changes in land use have been a major influence in these changes mainly afforestation and increased water use mainly for agriculture (Vaz and van der Zaag, 2003). With full development as allowed by the TIA total abstractions in the basin are expected to increase significantly and this will result in a severe decrease in river flow downstream in Mozambique and will impact negatively in the Incomati estuary (van der Zaag, 2008).

However, there are few known detailed studies attempting to investigate the contribution of land use changes and agricultural water abstraction on streamflow changes. A few examples are studies by Nkomo (2004) and LeMarie *et al.* (2006). This makes it difficult for policy makers to design realistic and suitable integrated water and land management interventions in the basin, which may result in unsustainable and inappropriate resource utilization. Therefore, this study addresses this gap in knowledge by giving an assessment of the effects of land use change and increased agricultural water use on the flow regime of the Incomati River in Mozambique, as these are the critical factors influencing the river flow dynamics in the basin.

1.2 Justification of the Study

The IncoMaputo Agreement was transitory and will end in 2012 as it had a ten year life-span. A final Agreement is expected to be reached in 2012 therefore studies similar to the current one are required to assist in the discussions of the permanent Agreement issues mainly regarding the reallocation of water among the three riparian states. In addition, this study will generate knowledge which could assist in catchment management and in designing strategies to minimize the impact of land use changes and increased water demand on river flow regime. It also represents an opportunity to implement the principles of IWRM in the basin which can improve the livelihoods of local communities, particularly those in the downstream part of the basin.

1.3 Objectives of the Study

1.3.1 General Objective

To assess the effect of land use change and increased agricultural water demand in the Incomati River flow regime in order to recommend appropriate IWRM practices to mitigate the aforementioned impacts.

1.3.2 Specific Objectives

1. To investigate changes in land use and agricultural water abstraction from 1990 to 2010 in the lower Incomati River basin;
2. To assess the changes in the river flow regime during the above mentioned period;
3. To relate the identified changes in land use and agricultural water use to the downstream river flow;
4. To verify whether the observed river flows at the upstream key gauge stations are in accordance to the optimal flows stipulated by the Tripartite Interim Agreement.

1.4 Research Questions

1. How has the land use and agricultural water abstractions changed in the Incomati River basin from 1990 to 2010?
2. How has the river flow changed during the same period and how significant are these changes?
3. Are the changes in the river flow regime related to land use changes and increased agricultural water abstraction?
4. Are the observed river flows at the key upstream gauge stations in accordance to the optimal flows stipulated by the Tripartite Interim Agreement?

1.5 Hypothesis

$H_{0:}$ There is no significant relationship between land use change and increased agricultural water use and the river flow regime in the downstream part of the Incomati River in Mozambique.

1.6 Thesis Layout

This thesis is structured into 6 chapters organised as follows: Chapter 1 presents the thesis introduction where background information, problem statement, justification of the study, objectives, research questions, research hypothesis and the thesis structure are presented. Chapter 2 presents the literature review mainly on the impact of land use changes on river flow regime. Chapter 3 gives the detailed description of the study area which includes the geographic location, physiographic characteristics, land use and land cover, climate, hydrology and water use aspects. The methodology employed for conducting the study is described in Chapter 4. Chapter 5 summarizes the work carried out and presents the evaluation and discussion of the results obtained. Finally, Chapter 6 outlines the conclusions drawn from this study and recommendations. Some suggestions for further work are also presented.

CHAPTER 2

2.0 LITERATURE REVIEW

2.1 Introduction

This chapter introduces the concepts of land use and land cover and their impacts on the river flow regime, the impact of water abstraction on river flow regime and the effect of land use change and water abstraction on river flow regime. This was done on the basis of existing literature and studies done in the region as well as in other parts of the world.

2.2 Overview of Land Use and Land Cover

Humans have been altering land cover since pre-historic times through the use of fire to flush out game and the clearance of patches of land for agriculture and livestock. In the past centuries the impact of human activities on the land grew enormously, altering entire landscapes, and ultimately impacting the earth's nutrient and hydrological cycles as well as climate (Sherbinin, 2002).

The term land use is used to describe human uses of the land, or immediate actions modifying or converting land cover. It includes such broad categories as human settlements, protected areas and agriculture (Sherbinin, 2002). Within those broad categories are more narrow categories, such as urban and rural settlements, irrigated and rainfed fields, national parks and forest reserves and transportation and other infrastructure. Schulze (2000) referred to land cover as the biophysical state of the earth's surface and its upper sub-surface. These are generally a reflection of the local climate and landforms, though they too can be altered by human actions. Examples of broad land cover categories include forest, tundra, savannah, desert or steppe (Sherbinin, 2002).

2.3 Effects of Land Use on Hydrology

The relationship between land use and hydrology is of greater interest worldwide as it can provide advice for management actions in order to avoid or minimize the negative effects of specific land use activities on the hydrology of a certain region. However, there are still uncertainties on the impact of specific land use practices to different processes of the hydrological cycle due to the complexity and specificity of characteristics of each catchment. Much of the present understanding of land use effects on hydrology is derived from controlled experiments and manipulations of the land surface coupled with observations of hydrological processes, commonly precipitation inputs and stream discharge outputs (DeFries and Eshleman, 2004).

According to Calder (1992), the largest changes in terms of land area, and arguably also in terms of hydrological impacts, often arise from afforestation and deforestation activities. One of the direct effects of land use changes on hydrology and hence on water resources is through its link with the evapotranspiration regime. Any change in land use and vegetation cover can have impacts on potential and actual evapotranspiration as well as on the discharge regime, which reflects the integrated behaviour of all the hydrological processes acting in the catchment (Zahabiyoun, 1999). The higher evapotranspiration loss from a forest than from any other land surface is the main reason for this situation (Lorup and Hansen, 1997).

2.4 Effects of Afforestation and Deforestation on Hydrology

The magnitude of changes on the streamflow due to land use changes varies with catchments and other factors such as climate and human activities. Regarding the impact of deforestation and afforestation on the dry season flow in the tropics, there are conflicting statements and findings. Edwards (1979) in an experiment conducted in Mbeya, observed that the dry season flow was higher from a catchment with traditional smallholder cultivation than with forest cover, even on steep slopes. Similar results were observed after deforestation of Brachystegia woodland in Zambia (Mumeka, 1986) and Montane hardwood forest in Taiwan (Hsia and Koh, 1983). In South Africa, afforestation of dry grassland and fynbo scrubland resulted in a highly significant decrease in low flows (Smith and Scott, 1992). Bosch and Hewlett (1982) suggested that forest cutting and removal activities usually cause increases in flood peaks for several years following disturbance, but some authors including Reinhart *et al*. (1963), Jones and Grant (1996), Whitehead and Robinson (1993) have suggested that these effects can be at least partially attributed to soil compaction during road and skid trail construction.

In the case of the Incomati basin, few detailed studies have been conducted to assess the impact of land use changes on river flow regime. Nkomo (2003) modelled the water resources in the basin using the WAFLEX model and observed that commercial afforestation, which is one of the major economic activities in the basin, created significant reduction of the natural runoff.

2.5 Effects of Agriculture on Hydrology

As is the case with afforestation and deforestation, the impacts of agriculture largely depend on catchment characteristics and local management activities in place. In general, a change in land use from natural vegetation to agricultural crops often results in a drop in interception rates, a rapid delivery of storm flow to streams, and a reduction in infiltration capacity of the soils due to compaction (Stipinovich, 2006). Another direct effect of agriculture on streamflow takes place through irrigation water abstraction, as large volumes of water are diverted from the river system, thus reducing the flows to downstream areas.

2.6 Effects of Water Abstractions on Flow Regime

Abstractions of water from surface and groundwater bodies for multiple uses including irrigation purposes affect the natural hydrological cycle. A reduction in discharge alters the width, depth, velocity patterns and shear stress within the river channel (Armitage and Petts, 1992). This can modify the distribution and availability of in-stream habitat with detrimental effects on invertebrates and fish populations (Wood *et al.,* 1999). Altered flow regimes have also been linked to invasion of non-native species (Brown and Moyle, 1997).

In the case of the Incomati River basin, economic developments resulting in increased water use have been tremendous since the 1970s (Sengo *et al.*, 2005). By the year 2002 total net consumptive water use was estimated at 1810 Mm^3/a or 51% of the average amount of surface water generated in the basin (Vaz and van der Zaag, 2003). Irrigation is the major water user, and by 2002 it was accounting for 48% of total water use (Sengo *et al.*, 2005) (Table 2.1). However the three Parties to the Tripartite Interim Agreement agreed to allow water use to increase through more irrigation and afforestation in Swaziland and South Africa to about 992 Mm^3/a (TIA, 2002). This is 69% of the mean annual runoff and it is a very high level of commitment for a catchment (Nkomo, 2003).

Table 2.1: Estimated consumptive water use (Mm^3/a) in 2002 in the Incomati basin, excluding evaporation losses from dams (source: Adapted from Vaz and van der Zaag, 2003)

Country	Water generated	Domestic and municipal	Industry	Livestock and game	Exotic tree plantations	Irrigation	Interbasin transfer	Total Consumption
South Africa	2937	90	35	8	473	670	132	1408
Swaziland	479	6	1	2	46	48	135	238
Mozambique	171	3	11	1	2	150	0	167
Total	3587	99	47	11	521	868	267	1813
% of the total use		**5.5**	**2.6**	**0.6**	**28.7**	**47.9**	**14.7**	

Upstream developments have reduced the amount of fresh water that reach the Incomati estuary, thus, modified the estuary's flow regime in Mozambique (LeMarie *et al.*, 2006). The Tripartite Interim Agreement, among others, recognizes the water requirements for the environment, and in the absence of more precise information, some minimum target environmental flows have been set. As the final Agreement is scheduled to be reached by end of 2012, it is important that Mozambique monitors the river flow regime downstream of the Incomati basin, including the ecological state of the river, particularly in the estuary. This can allow assessing the adequacy of the approved optimal flows, particularly those entering the Mozambican border, and the feasibility of further permitted developments.

2.7 The Combined Effect of Land Use Change and Water Abstraction on River Flow Regime

The river flow regime in a catchment is sensitive to many factors, some of which have been significantly researched e.g. climate changes and land use. However, there are few studies done which attempt to combine the various factors and present their impact on the river regime. This may be due to the complexity of the exercise but also may be due to relatively poor understanding of the whole system as suggested by Lorup and Hansen (1997).

Advances made by Gao and Yang (2008) allowed modelling of the combined effect of different factors on the flow regime, and the approach was based on a distributed geomorphologically based hydrological model (GBHM), capable of fixing one factor and changing the other to model its influence on regime flow separately. Another study done by Stipinovich (2005), looked at change in land cover and water abstraction in the Bot River catchment in South Africa using a combination of rainfall-runoff Pitman SHELL model with GIS techniques. The study failed to make direct links between some factors and the impact in runoff due to the complexity involved in the modelling process.

In the case of the current study, a model applying a similar principle to the GBHM model is proposed to be used in order to investigate the impact of land use change and increased agricultural water use in the Incomati basin. The model will be combined with statistical analysis and GIS in order to complement the whole data analysis process as explained in chapter 4.

2.8 The Use of Hydrological Modelling in Assessing Land Use Changes Impacts

Many models have been used to assess impacts of land use and water abstractions on the hydrology. The choice of one or the other depends on many factors which may vary from model and data availability to the complexity and expertise required by each model. Some examples of models used in investigating the impact of land use changes on hydrology include: GBHM, Pitman based SHELL model and TOPMODEL. The applicability of each of the aforementioned models in assessing the effects of land use change on hydrology is discussed below.

a) Geomorphologically Based Hydrological Model (GBHM)

It is a fully distributed physical hydrologic model developed for simulation of regional watershed hydrology using digital elevation models (DEMs). The model employs area and width functions to lump the topography and divide the catchment into a series of flow intervals. Spatial parameters are averaged over each flow interval and represented by one-dimensional distribution functions (Alam *et al*., 2011).

According to Alam *et al*. (2011), the model's advantages and disadvantages can be summarized as follows;

Strengths

- The model is also flexible in describing other spatial variability, such as land-cover and soil-type;
- Its runoff generation mechanism is more accurate in comparison with other models such as GBHM, MIKE SHE and the TOPMODEL;

- Human activities for water resources assessment and management in large river basins can be incorporated in GBHM.

Drawbacks

- The model requires high computational power since the whole catchment is considered for the simulation;
- Not freely available for use.

b) Pitman-based SHELL Model

This is a container model within which runs the Pitman model component that accounts for all natural factors and the separate attached sub-models that account for the effect of various land cover types (Stipinovich, 2005).

According to Stipinovich (2005), the model's advantages and disadvantages can be summarized as follows:

Strengths

- The model is relatively simple in its approach;

Drawbacks

- It is difficult to calibrate as it requires relatively good hydrological and modelling expertise;
- Its application can be time consuming and expensive as it runs with other attached sub-models.

c) TOPMODEL

Is a semi-distributed model which has a simple representation of basin characteristics and hydrologic processes (Beven, 1997b) as compared to fully distributed and data demanding models like MIKE SHE (Refsgaard and Storm, 1995). The model is applied to simulate outflows from catchments and to predict spatial and temporal soil moisture dynamics and variable source areas in space and time (Ambroise *et al*., 1996).

According to Beven (1997b), the following are the model strengths and drawbacks to be considered when using the model.

Strengths

- The model is simple and versatile with major advantages in its parametric parsimony and the capability to visualise the simulation results in a spatial context;
- The model is free for use in research and education purposes.

Drawbacks

- The model includes some assumptions, like the exponential behaviour of the saturated zone, the water table surface parallel to the ground and the constant upslope contributing area, which cannot be always safely accepted;
- The physical interpretation of calibrated parameters can be difficult.

The TOPMODEL has been used in previous studies such as by Gumindoga (2010) in the Upper Gilgel Abay River Basin to model the hydrological impacts of land use changes and by Chairat and Delleur (1993), with modifications, to consider the effects of drainage systems in agricultural watersheds in north central Indiana. The TOPMODEL performed well in both cases.

In this work, Geospatial Stream Flow Model was selected due to the fact that it is user friendly and capable of performing the required analysis as explained in detail on section 2.7.

2.9 The Geospatial Stream Flow Model (GeoSFM)

The USGS GeoSFM is a physically based semi-distributed geospatial hydrologic model. It was developed to establish a common visual environment for the monitoring of hydrologic conditions over wide areas (Artan *et al.,* 2001). The model operates as an extension within ArcView 3.2 and therefore requires data in GIS formats. Remotely sensed, ground observation (soil, land cover, rainfall and evaporation) and digital elevation data sets describing the land surface are the main input required by the model to calculate the basin hydrological water cycle (Artan *et al.,* 2001). GeoSFM provides a continuous simulation of stream flow, on a daily time step, providing a stream flow forecasting for the next 3 days. The model consists of two parts: a GIS-based module used for model data input and preparation, and the rainfall-runoff processing module (Mutie *et al.*, 2006) (Figure 2.1).

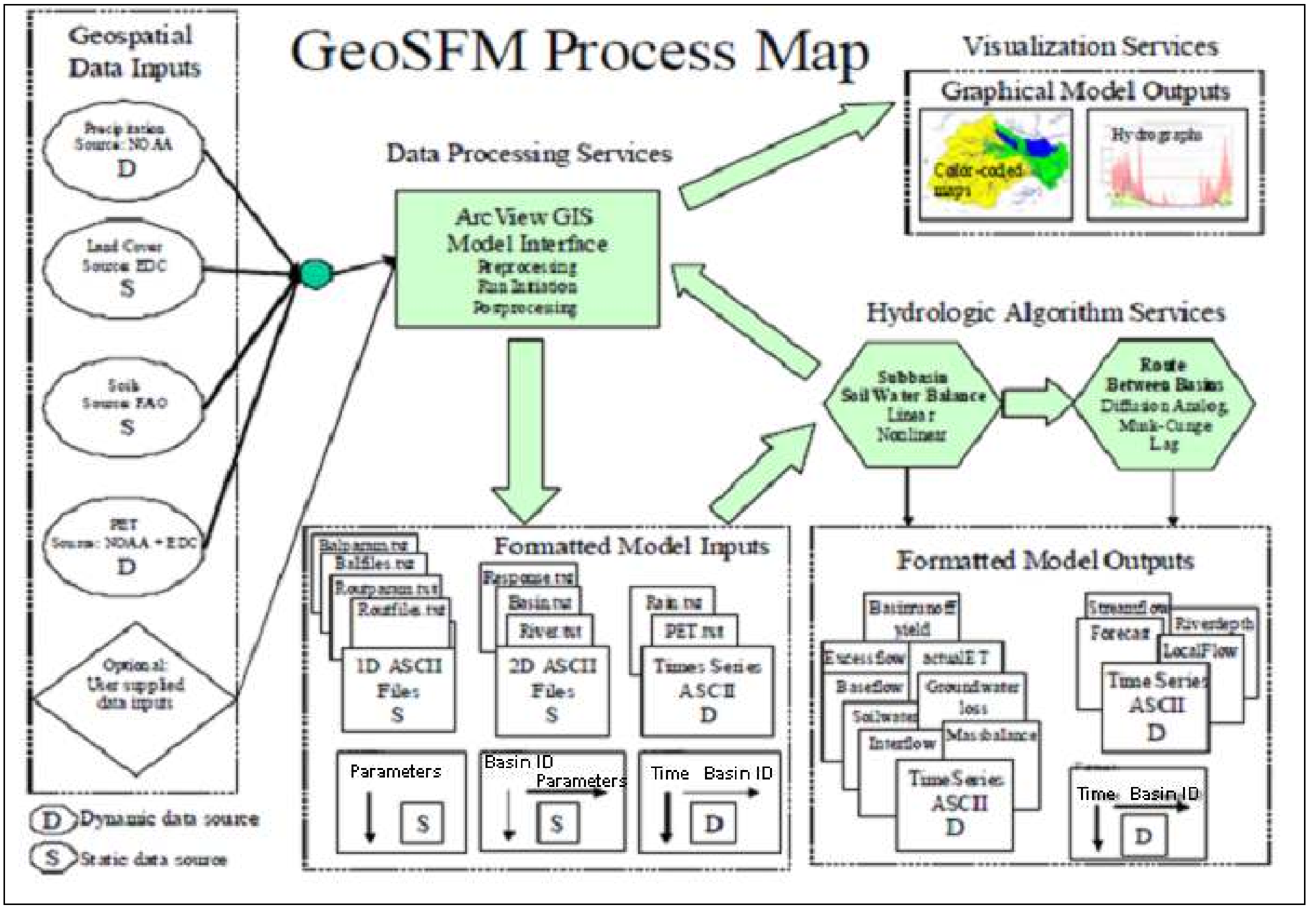

Figure 2.1: Schematisation of the GeoSFM conceptual structure (Asante *et al.,* 2008).

Most of the data required in the model are raster grids, and the spatial nature of raster grids requires the adoption of a customizable geographic information system with excellent raster functionality (Vilanculos, 2006).

In terms of strengths and weaknesses of the model, the following can be underlined according to Entenman (2005), Guleid *et al.* (2004) and USGS (2008):

Strengths:

- Use of global data sets that cover the whole African continent;
- Rainfall data is derived from freely available satellite images;

- The model is suitable for wide-area application in data scarce environments unlike most hydrologic models commonly used nowadays which are unsuitable for this condition;
- The model is free, relatively easy and cheaper to implement.

Drawbacks:

- The model is difficult to calibrate and run;
- Data processing can be time consuming.

2.10 Previous Experiences in the Use of the Geospatial Stream Flow Model

The GeoSFM has been applied successfully in many parts of Africa. Mutie *et al.* (2006), conducted a study to evaluate land use change effects on river flow using USGS Geospatial Stream Flow Model in Mara River basin in Kenya. There were reports of land use changes in the upper part of the basin with far reaching consequences for the long-term sustainability of the natural resource base. Three different periods (1973, 1986 and 2000) were analyzed in order to detect changes on land use which later could allow simulating the impacts in terms of river flow. Simulation results with the model showed that land cover data from the year 2000 produced higher flood peaks and faster travel times compared to the 1973 land cover data. The changes detected indicate the effects of land use pressure in the basin.

Other known studies done using the model have been mainly in flood simulation. Examples are studies done by Vilanculos (2006) on the Olifant subcatchment in the Limpopo River Basin, where the model was integrated with GIS and ground observations to simulate and forecast floods in terms of their magnitude, travel time and impacts. The model was also applied by Mutua and Klik (2007) in predicting daily streamflows in the ungauged Masinga catchment, in Kenya and the results gave a model performance coefficient of 0.74 based on the Nash-Sutcliffe statistical criterion.

All these examples show the potential of Geospatial Stream Flow Model as a decision supporting and day-to-day management tool. By being a physically based semi-distributed geospatial hydrologic model it can be adjusted to be applied in a number of hydrological studies with a high degree of certainty.

In this study the model was integrated with GIS, remote sensing and statistics to assess impacts of land use changes and agricultural water abstraction on river flow regime, so as to produce useful information that can be used in catchment management and in decision making.

2.11 Major Points from Literature Review and their Relevance to the Study

Land use change is primarily a direct effect of human interventions though climate can play an important role that need to be always acknowledged when attempting to understand the whole cycle of changes. In general, there is an agreement between different authors on the fact that the largest changes in terms of land area and hydrological impacts, often arise from afforestation and deforestation activities. However, there are still uncertainties on the impact of specific land use practices to different processes of the hydrological cycle due to the complexity and specificity of each catchment. There are conflicting findings in terms of hydrological effects due to afforestation and deforestation, but most authors suggest that the former results in a decrease of low flows while the latter often results in increased peak flows. Agriculture has been associated with increase in interception rates, rapid delivery of storm flow to streams and a reduction in infiltration capacity of the soils due to compaction.

In the Incomati River basin, studies attempting to assess specific effects of land use change are few. Hence, the combined effect of most land uses on hydrological response of the basin is not well understood. This shows a gap in knowledge and it becomes even more critical when considering that water resources in the basin are already fully committed.

The existing literature allowed comparison of existing models to specifically deal with the effect of land use change on streamflows. GeoSFM was found to be the most suitable as it is a physically semi-distributed model, which means that it accounts for the spatial heterogeneity of the physical features under investigation. In addition, the model is free and performs well even in data scarce environments.

CHAPTER 3

3.0 DESCRIPTION OF THE STUDY AREA

3.1 Introduction

The selection of the study area was based on many factors, the first one being the fact that the basin is of strategic importance for Mozambique as it holds some of the major investments in the agricultural and energy sectors and its water resources are already fully allocated. Other factors include data availability, lack of similar studies in the area and the already visible phenomenon of salt intrusion from the Indian Ocean which is related to changes in flow regime. Details of the study area in terms of location, physiographic characteristics, hydrology and land use are presented in the coming subsections.

3.2 Location

The Incomati River basin is located in the south-eastern part of the African continent and covers a land area of about 46,700 Km^2 (Figure 3.1). It occupies 2,500 Km^2 of the Kingdom of Swaziland, 15,600 Km^2 of the Republic of Mozambique, and 28,600 Km^2 of the Republic of South Africa (Vaz and van der Zaag, 2003). The headwaters of the Incomati River are situated in the mountain and plateau area near Breyten in Mpumalanga Province, South Africa at about 2,000 m above sea level. Running generally eastward, it descends from the plateau, cuts a 900 m deep valley in north western Swaziland before reaching the Libombos mountains, where it is joined by the Crocodile River and through a valley (Komatipoort) in the Libombos mountains before entering Mozambique. Downstream of Komatipoort, the Incomati River flows north, in a great loop, spreads into Lago Chuáli, turns southward to reach the sea to the northeast of Maputo. The river is perennial. Three of the main tributaries of the Incomati, namely the Komati, Crocodile and Sabie, originate in the same area as the main river (Government of Mozambique, 2003). Other tributaries of the basin include; Massintonto, Uanetze and the Mazimechopes (Vaz and van der Zaag, 2003).

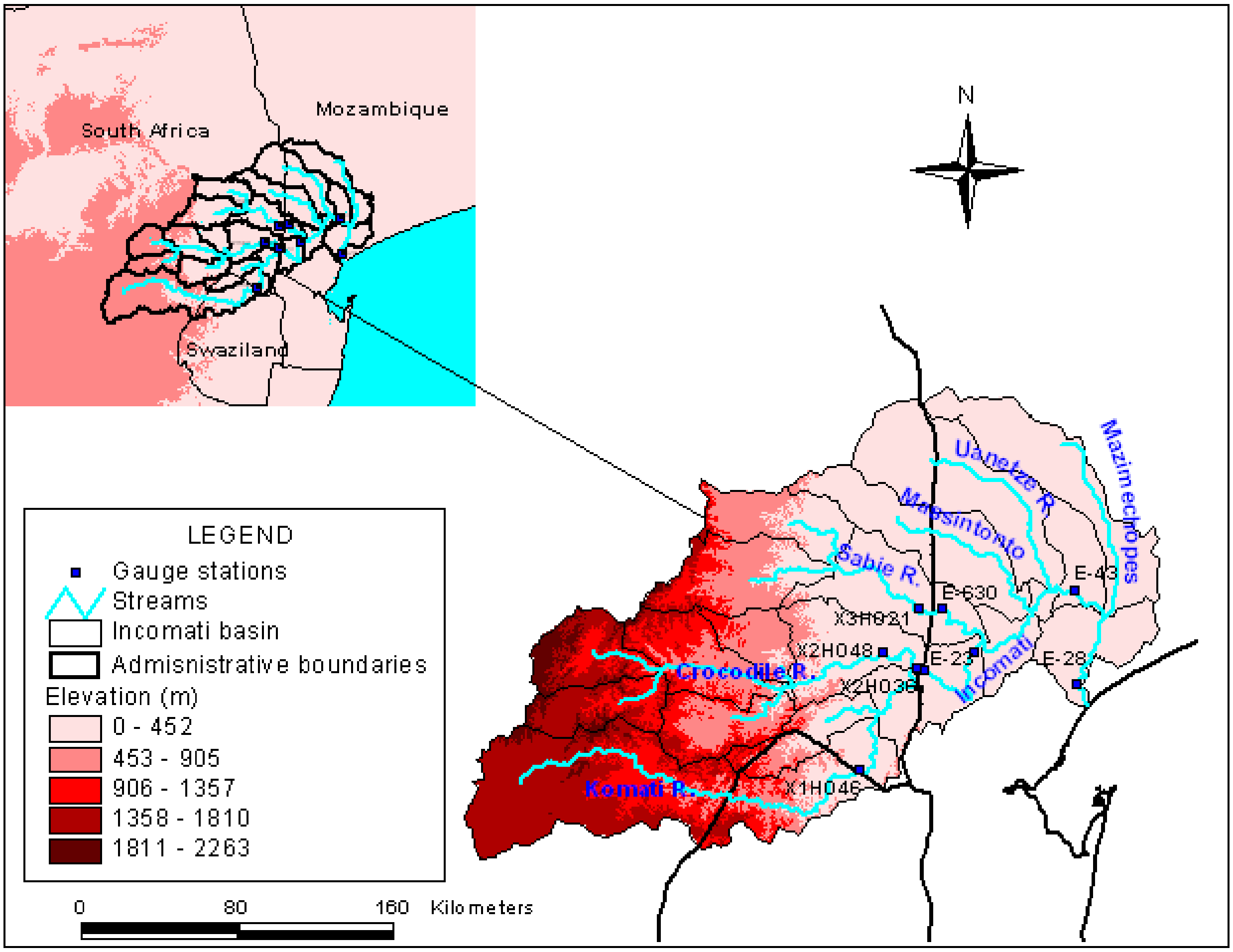

Figure 3.1: Location of the study area

3.3 Physiographic Characteristics

3.3.1 Topography

The altitude in the basin ranges from 2,263 m above sea level in the South African part to 0 m at the Mozambican part of the basin towards the coast (Figure 3.1). In terms of slope, the basin follows the same pattern as altitude, where high values of slope (25 degrees) occur in the upstream part of the basin in South Africa and as moving towards the coast it approaches zero. This topographic pattern makes the lower part of the basin prone to salt intrusion and flooding as a large area of the basin is close to sea level.

3.3.2 Soils

The soils of the basin vary in terms of type, depth and texture, largely due to the complex geology of the region, varied relief and rainfall gradients. The soils in the upper parts of the Komati, Crocodile and Sabie catchments are predominantly strongly weathered acid soils with clay-enriched sub-soils (Acrisols). Shallow Leptosols, deep, intensely weathered Ferrasols and deep, erosion-prone Lixosols overlay the escarpment and its foothills in the middle Komati and Crocodile catchments. Towards the east, the Lower Crocodile and Sabie catchments are overlain by unconsolidated Regosols. In the Libombo Range, Nitisols and Leptosols are very shallow, overlay hard rock, and are generally considered to be non-arable. Most of the Mozambican portion of the basin is covered by deep, transported sandy soils of marine and aeolion origin (Arenosols) with low fertility. Fertile alluvial deposits (Fluvisols) are found in the floodplains (TPTC, 2010).

a) Texture

Major part of the basin is composed of loamy soils (FAO, 1998). Other types include sandy, clay and basaltic soils (Figure 3.2).

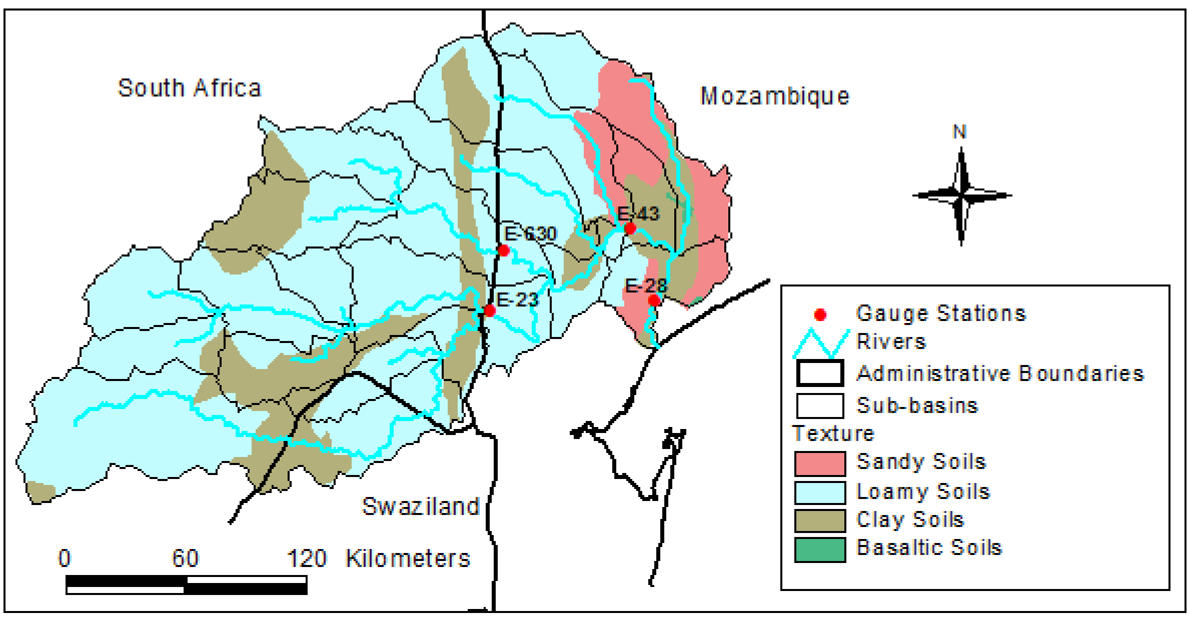

Figure 3.2: Spatial distribution of soil texture
Source: Adapted from United Nations Food and Agriculture Organization (1998)

b) Soil Depth

Based on the global data set of digital soil maps from FAO, the most predominant soils in the basin are moderately deep with moderate infiltration capacity. Other soils are deep and shallow with high and low infiltration capacity, respectively (Figure 3.3).

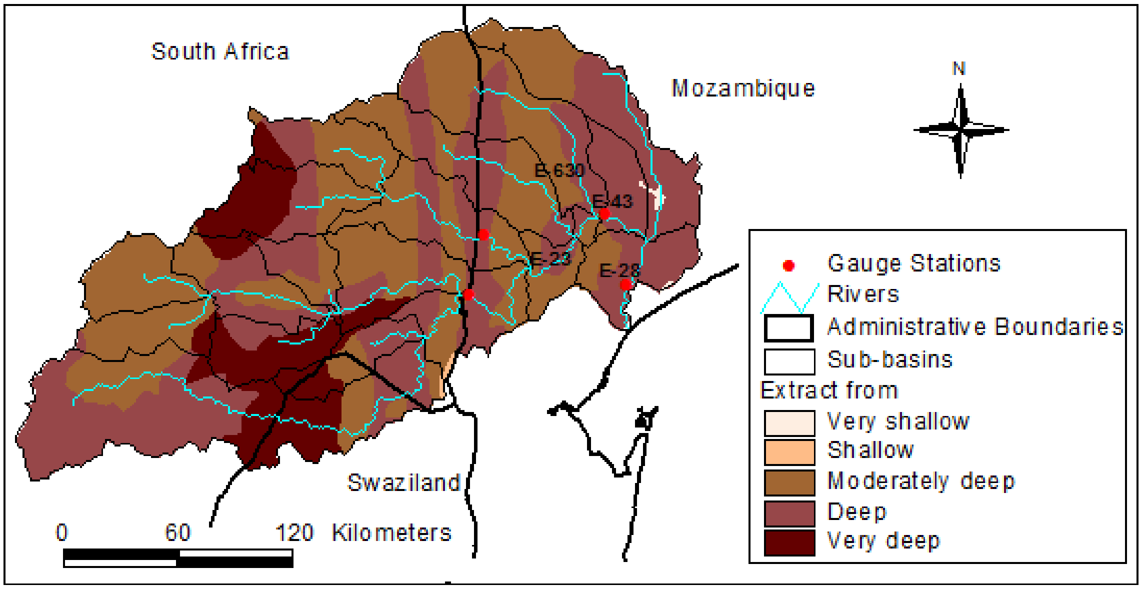

Figure 3.3: Spatial distribution of soil depth
Source: Adapted from United Nations Food and Agriculture Organization (1998)

3.3.3 Land Use and Land Cover

According to TPTC (2010), the dominant vegetation cover in the Incomati basin is the savannah. It covers more than 50% of the basin area. Towards the coast, the evergreen forest becomes the dominant land cover type (Figure 3.4). On the other hand, irrigated agriculture and commercial afforestation are the main water intensive land uses in the basin.

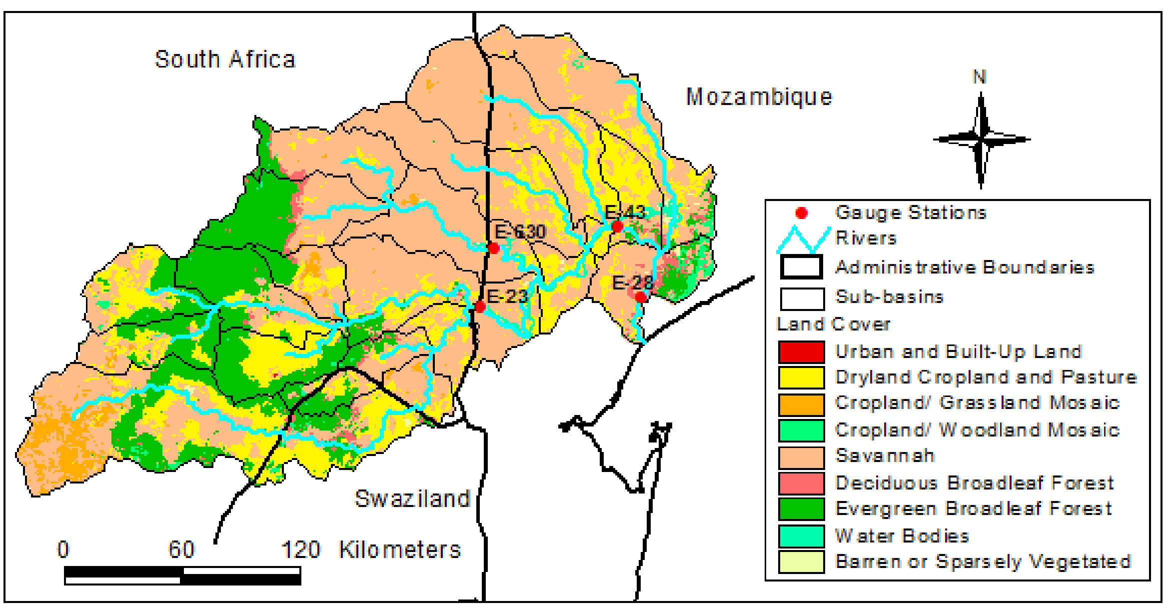

Figure 3.4: Spatial distribution of land cover
Source: Adapted from TPTC (2010) and USGS (2006)

3.3.4 Climate

Description of the climatic relevant variables of the study area is presented below. These variables include temperature, evapotranspiration and rainfall. They are determinants mainly of the runoff generation process. The climate of the Incomati River basin varies with the varied geography of the basin, from a warm and humid climate in the Mozambique coastal plain and lowveld, to a cooler dry climate in the South African highveld (TPTC, 2010).

a) Temperature

The mean annual temperature in the basin varies from about 22.5°C in the Mozambique Coastal Plain in the east of the basin to about 15°C in the South African highveld in the southwest of the basin (JIBS, 2001).

b) Rainfall

The rainy season in the Incomati basin lies between October and March, with the lowlands prone to tropical cyclones. The mean annual rainfall is about 740 mm/a, which increases from east to west. The highest rainfall occurs in the upper Sabie (around 1,200 mm/a) (Vaz and van der Zaag, 2003).

c) Evapotranspiration

The mean annual potential evaporation for the basin as a whole is 1,900 mm/a and generally decreases from east to west, resulting in an increasing deficit between rainfall and potential evaporation from west to east, and higher demands for irrigation towards the east (Sengo *et al.*, 2005). The lowest evapotranspiration values are found at the South African and Swaziland parts of the basin, where the mean annual values range from 1,467 mm/a to 1,537 mm/a. The highest values (around 1,817 mm) are found at the Mozambican part of the basin, near the coast (USGS, 2001).

Table 3.1 shows the most recent climatic characterization of the basin by TPTC (2010), in which the basin is divided into three zones, the escarpment, lowveld and Coastal plain.

Table 3.1: Summary of the Climate of the Incomati Basin

Zone	Rainfall (mm/a)	Temperature (^{o}C) Mean annual	Evaporation (mm/a)
Escarpment	800 to 1,200	10 to 16	1,600 to 2,000
Lowveld	400 to 800	14 to 22	2,000 to 2,200
Coastal Plain	401 to 800	20 to 26	2,200 to 2,400

3.4 Hydrology and Water Use

a) Surface Water

JIBS (2001) estimated the total net virgin runoff in the basin at 3,587 Mm^3/a, of which 82% is generated in South Africa, 13% in Swaziland and 5% in Mozambique (Table 3.2). About 80% of all runoff in a hydrological year is generated during the months November–April. Variations of discharge from year to year are significant, with floods and droughts occurring regularly, and the coefficient of variation of annual discharges is 50–65% (Vaz and van der Zaag, 2003).

Table 3.2 Water generation in the Incomati basin, by country (Source: JIBS, 2001)

Country	Catchment area (km^2)	%	Virgin discharge (Mm^3/a)	%
South Africa	28,556	61	2,937	82
Swaziland	2,545	5	479	13
Mozambique	15,647	33	171	5
Total	**46,748**	**100**	**3,587**	**100**

The Incomati Water Availability Assessment Study (IWAAS) by DWA (2009), is the most recent and most thorough hydrological analysis undertaken in the South African and Swazi parts of the basin, while the latest hydrology within the Mozambican part of the catchment is that of the Three Basins Study (TPTC, 2010). Table 3.3 shows the summary of the hydrology of the Incomati basin based on different studies.

Table 3.3: Hydrology of the Incomati Basin (TPTC, 2010)

Catchment	Contribution to MAR (million m^3/annum) (1925 to 2000)							
	Mozambique		Swaziland		South Africa		Total	
	IIMA	TPTC (2010)	IIMA	TPTC (2010)	IIMA	TPTC (2010)	IIMA	TPTC (2010)
Komati			475	488	975	844	1,450	1,332
Crocodile					1,225	1,124	1,225	1,124
Sabie	0	7			750	661	750	668
Massintoto	10	21			10	20	20	41
Uanetse	10	19			5	14	15	33
Mazimechopes	20	20					20	20
Incomati	130	258					130	258
TOTAL	**170**	**325**	**475**	**488**	**2,965**	**2,663**	**3,610**	**3,476**

Upstream developments in the basin have been significant and their impacts have been remarkable, especially in the downstream part of the catchment. Figure 3.5 show a comparison between a pristine condition (before 1980) and a developed condition of the basin (after 1980) at Ressano Garcia in Mozambique near the border with South Africa.

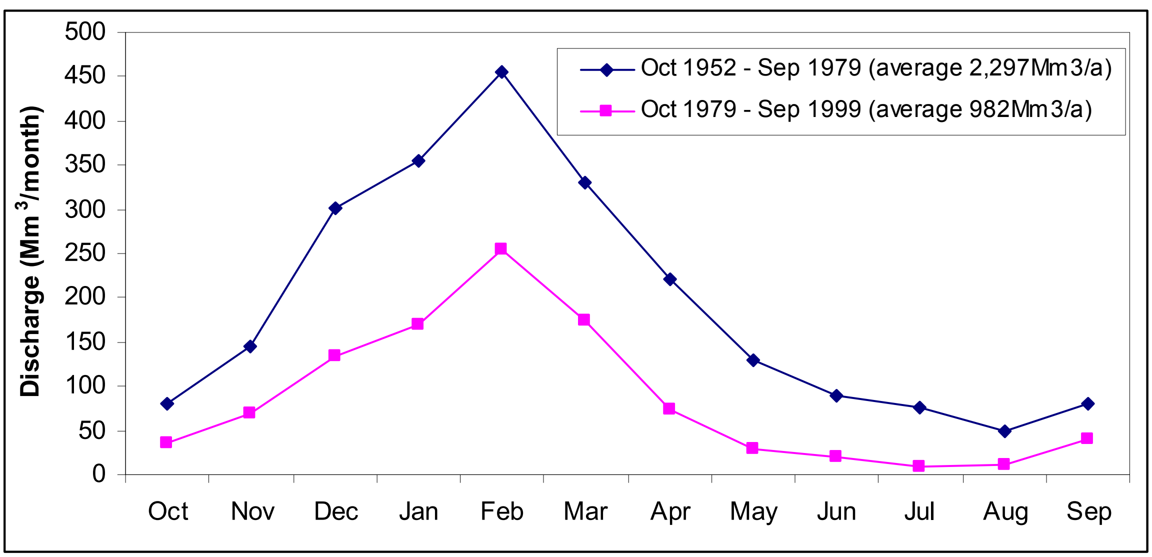

Figure 3.5: Average discharge of the Incomati at Ressano Garcia (station E-23); 1953–1979 and 1980–1999. (Source: adapted from Vaz and van der Zaag, 2003).

b) Ground Water

Groundwater occurs in sufficient quantities for large-scale development only in the dolomites of the Transvaal Sequence, the Barberton Greenstone Belt, the alluvium of the Incomati river valley in the Mozambique coastal plain (with an estimated rate of recharge of about 150 Mm^3/a), and in the aeolian sands in the east of the Mozambique coastal plain (recharge is about 29 Mm^3/a) (Vaz and van der Zaag, 2003).

3.4.1 Water Use

By far the largest water user in the Incomati River Basin is irrigation, followed by commercial forestry. Other water uses, such as domestic and industrial use, have increased gradually over the years with industrial water use, being driven mostly by the sugar industry (TPTC, 2010).

a) Irrigation

Since 1991, there has been significant growth in irrigation in the Lower Komati due to the construction of the Maguga and Driekoppies Dams, which has increased the assurance of supply for farmers. Irrigation in the other parts of the Komati has remained relatively stable (DWA, 2009). There has been significant growth in irrigated areas (40% to 60%) in the middle Crocodile and Lower Crocodile catchments. This has happened at the expense of irrigation in the Upper Crocodile, which has declined by about 35% over the same period. This is due to trading of water rights to downstream users (DWAF, 2009). Irrigation has grown significantly in the Sabie and Sand drainage areas since the mid-1980s. There is no irrigation in the Lower Sabie catchment which is located within the Kruger National Park (TPTC, 2010).

In the Mozambican part of the basin, irrigated sugarcane is cultivated in the medium and lower or coastal parts of the basin. Irrigation development started around 1910 with the establishment of the sugarcane plantation and sugar mill at Xinavane. The area of sugarcane peaked at about 260,000 ha in 1975 and then declined to about 7,500 ha in 1993 due to the civil unrest. A rehabilitation program for the mill and estates commenced in 2000 and the irrigated area in 2004 was estimated to be about 17,700 ha (Table 3.4) (DWA, 2009).

Table 3.4: Historical land use in the Incomati basin (DWA, 2009)

River sub-catchment	Area of sugarcane (ha)		Area of commercial timber plantations (ha)		Irrigated crops other than sugarcane (ha)	
	1985-93	**2004**	**1985-93**	**2004**	**1985-93**	**2004**
Komati	22,830	38,942	97,000	120,300	7,209	12,297
Crocodile	18,730	25,535	199,600	194,100	18,730	25,535
Sabie	-	-	72,500	85,300	8,180	12,760
Incomati in Mozambique	7,500	17,700	-	-	-	-
TOTAL	**49,060**	**82,177**	**369,100**	**399,700**	**34,119**	**50,592**

b) Water Transfers

Large volumes of water (around 104.7 Mm^3/a) are transferred out of the basin, from the Nooitgedacht and Vygeboom Dams, and the Gemsbokhoek weir to power stations within the upper Olifants River basin in South Africa. Transfers also take place from the Komati River in Swaziland to the Mbuluzi catchment for irrigation (121.8 Mm^3/a) (Vaz and van der Zaag, 2003).

There are no major transfers into or out of the Incomati catchment in Mozambique. There are plans for future water transfers out of the catchment, near the town of Moamba or at the confluence with the Sabie River, for urban water supply of Maputo. About 90 Mm^3/a will be required for this purpose (TPTC, 2010).

CHAPTER 4

4.0 MATERIALS AND METHODS

This study was conducted through field visits and desk studies using short-term historical streamflow, rainfall and evaporation data, historical data of water usage by agriculture in the basin, Landsat images for Incomati, GIS layers of different features such as stream networks, reservoirs, gauge stations and other relevant spatial data of the Incomati basin. Field visits were done to confirm some of the features on the ground. This section describes in detail the methods employed in the study which are summarised in the diagram below (Figure 4.1).

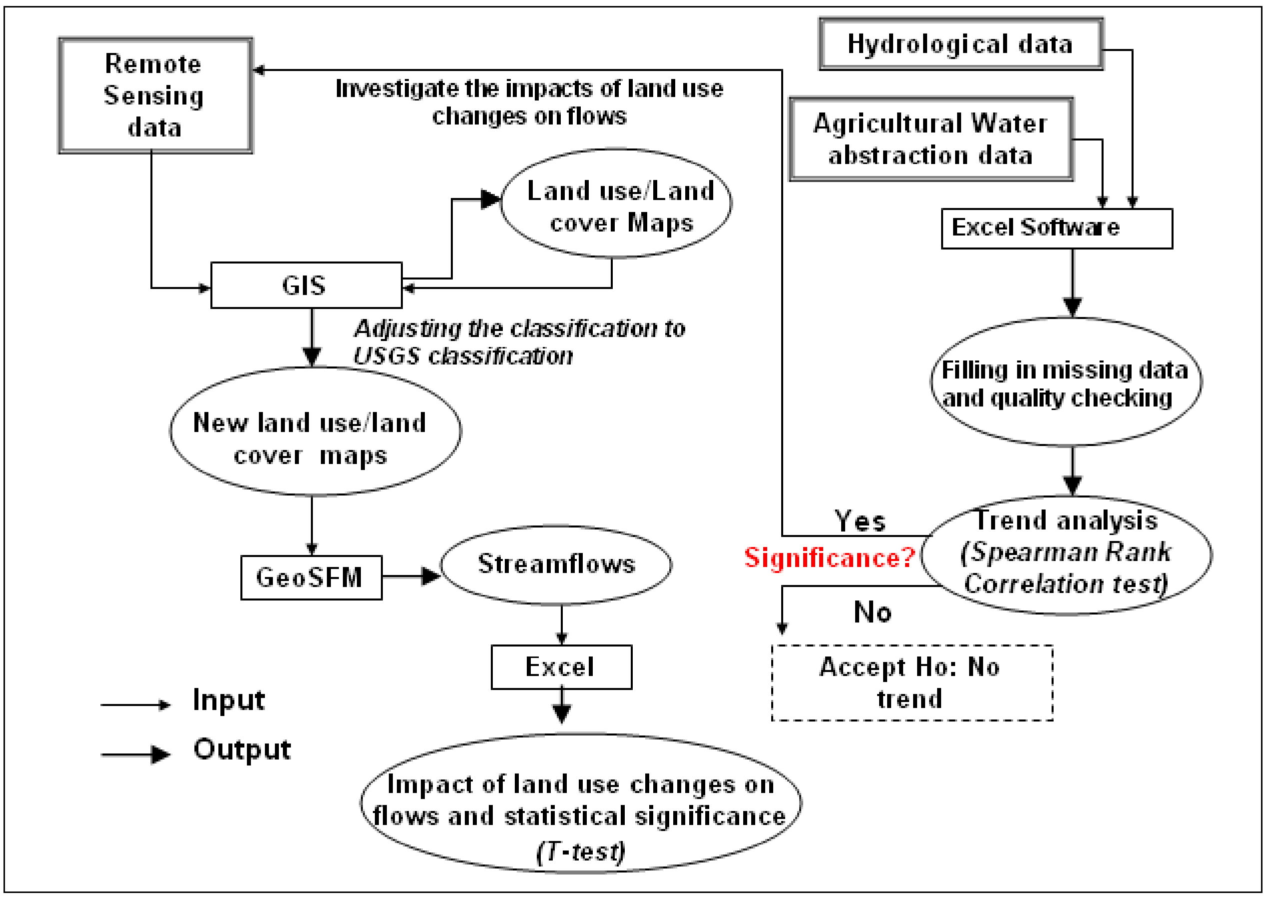

Figure 4.1: Summary of study methods

4.1 Data Availability and Acquisition

4.1.1 Landsat TM Images

The Landsat TM images used in this study were acquired from three sources, namely: the United States Geological Survey Global Visualization website http://glovis.usgs.gov/, the Landsat.org website http://landsat.org/ortho/index.php and Mozambican National Centre of Remote Sensing and Cartography (CENACARTA). These data were used in mapping land use and land cover changes in the basin. Appendix B presents the table indicating Landsat images used in this study.


http://glovis.usgs.gov/,

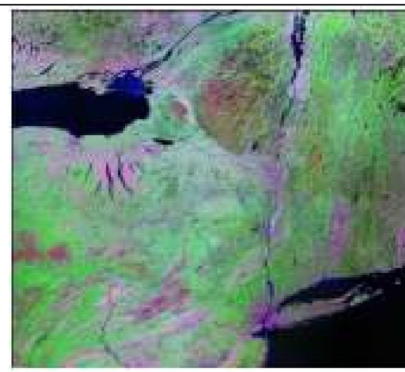
http://landsat.org/ortho/index.php

Figure 4.2: Landsat images and the corresponding acquisition websites

4.1.2 Water Use Data

Historical agricultural water use data were obtained partly from updated studies in the basin (PRIMA, 2010; DWAF, 2009). Another part of these data were acquired from the water management institutions in the 3 countries, namely ARA-Sul in Mozambique and Departments of Water Affairs of Swaziland and South Africa. The data were provided in terms of irrigated areas and in order to have the corresponding volumes of water a transformation equation was used which was derived from studies of the average water demand by agriculture in the basin taking into account the prevailing climatic and soil conditions (Equation 4.1).

$$AWU = 10{,}000 * Ir.area \quad \text{......Equation 4.1}$$

Where:

AWU - Annual Agricultural Water Abstractions (m^3);

Ir.area - total irrigated area (ha).

These data were used to examine agricultural water use trend and its significance in the basin since 1990.

4.1.3 Observed Hydrological and Weather Data

Observed hydrological and weather data as shown in tables 4.1 and 4.2 (runoff and rainfall) was obtained from the water management entities of the three countries, ARA-Sul in Mozambique and DWAs' of South Africa and Swaziland. Observed rainfall data were used to validate the satellite-derived rainfall data used as the main input in the modelling. Observed runoff data were used to investigate the streamflow changes and their magnitude in the basin, validation of the model results and in the model calibration process.

Table 4.1: Observed rainfall data used in the study

Station Code	Station Name	Temporal Coverage
P-856	Ressano Garcia	1991/92 to 2009/10
P-589	Magude	2000/01 to 2003/04
P-63	Manhiça	2000/01 to 2003/04
0596179	Skukuza	1987/88 to 2009/10
0520450	Mananga	1969/70 to 2009/10
0557712	Krokodilburg	1955/56 to 2009/10

Table 4.2: Observed runoff data used in the study

Station Code	Station Name	Temporal Coverage
E-23	Ressano Garcia	1952/53 to 2009/10
E-43	Magude	2000/01 to 2003/04
E-630	Corumana dam	1989/90 to 2009/10
X3H015	Lower Sabie	1987/88 to 2009/10
X1H003	Tonga	1954/55 to 2009/10
X2H016	Tenbosh	2002/03 to 2009/10
X1H001	Hoogenoeg	1954/55 to 2009/10
X1H036	Downstream of Vygeboom Dam	1971/72 to 2009/10
X1H046	Mananga	1978/79 to 2009/10
X3H021	Kruger Gate	1990/91 to 2009/10
X3H008	Exeter	1987/88 to 2009/10
X2H006	Karino	1955/56 to 2009/10
X2H022	Dolton	1959/60 to 2009/10
X2H046	Riverside	1985/86 to 2009/10

4.1.4 GIS Layers

GIS layers of different features such as flow and rain gauge stations, dams/reservoirs, stream networks, sub-basins, irrigated fields and others were acquired from ARA-Sul in Mozambique, SRK Consulting Engineers and Scientists in South Africa and from the website of the Department of Water Affairs of South Africa, www.dwaf.gov.za. These data were used in mapping different physiographic features used in the characterization of the study area and in the presentation of the study results.

4.1.5 Data for Modelling

Most of the data required to run the GeoSFM were obtained from various websites as described below.

a) Satellite Rainfall Estimate (RFE) data

This is the most important data required to run the Geospatial Stream Flow Modelling and were the driving factor in the design of the model (Asante *et al.*, 2008). The model uses this data to simulate daily amount of streamflow to be generated in each catchment. This data is provided by United States National Oceanic and Atmospheric Administration Climatic Prediction Centre (NOAA) and by United States Geological Survey at a daily base and was downloaded from http://edcdaac.usgs.gov/adds/africa. The satellite rainfall data used in this study was for the period 2000 to 2004.

b) Potential Evapotranspiration (PET)

This represents atmospheric demand for water from the earth's surface as a function of solar radiation, air temperature, wind, humidity and atmospheric pressure. PET was used in daily basin water balance on a cell-by-cell basis according to the Penman-Monteith equation as recommended by Entenman (2005). Grids are produced on daily time step for use within the model. The PET data used in this study were for the period 2000 to 2004 and were downloaded from http://edcdaac.usgs.gov/adds/africa.

c) Digital Elevation Model (DEM)

This data is a basic input of the basin delineations, stream networks, bearing topological identification numbers, as well as grids of flow direction, flow accumulation, slope and other variables. The 1 km resolution HYDRO1k DEM produced at USGS EROS is used in GeoSFM because of its global coverage. HYDRO1k is a hydrologically corrected DEM, which implies that it is devoid of spurious pits that interrupt hydraulic connectivity over the land surface (Asante *et al.,* 2008). The DEM was downloaded from http://edcdaac.usgs.gov/gtopo30/hydro and it provides the spatial framework for the model.

d) Soil Data

The Digital Soil Map of the World (DSMW) produced by United Nations Food and Agricultural Organization is the data set that was used in the study because it is the finest resolution soil database with global coverage freely available. The Geospatial Stream Flow Model requires soil data to set hydraulic parameters that govern interflow, soil moisture content and deep percolation to the groundwater table. The soil data are required to describe soil parameters such as average water holding capacity of the soil in millimetres, average hydrologic active soil depth in centimetres, textual description of the average saturation soil hydraulic conductivity (m/h), average Soil Conservation Service (SCS) curve number for the soils and minimum and maximum percentage of the watershed which can be impervious for each sub-watershed makes up the watershed being modelled. The data was downloaded from ftp://daac.gsfc.nasa.gov/data/.

e) Land Use and Land Cover Data

The data was downloaded from http://edcdaac.usgs.gov/glcc/af_int.html. The data is needed to determine the response of the watershed being modelled to rainfall events. The land use and land cover data together with soil data determine the response coefficients used in the Geospatial Stream Flow Model to determine the amount of excess precipitation, recharge to the groundwater system and the amount of water held in storage in the soils.

United States Geological Survey (2006) classified soils into four hydrologic soil groups according to their infiltration rate:

- Group “A” consists of soils that have low runoff potential and high infiltration rates; the soil textures included in this group are: sand, loamy sand and sandy loam. The transmission rates of these soils are greater than 0.76 cm/h;
- Group “B” consists of soils that have moderate infiltration rates. The soil textures included in this group are silt loam and loam. The transmission rates of these soils are between 0.38 and 0.76 cm/h;

- Group “C” consists of soils that have low infiltration rates. The soil texture included in this group is sandy clay loam. The transmission rates of these soils are between 0.13 and 0.38 cm/h; and
- Group “D” consists of soils that have very low infiltration rates. The soil textures included in this group are clay loam, silty clay loam, sandy clay, silty clay and clay. The transmission rates of these soils are between 0.0 and 0.13 cm/h.

From these four soil groups, numeric values were given to ease the grid creation process. The Numeric Soil Hydraulic classes, found in the last column, are used when creating the RCN grid.

In this study the downloaded land use/ land cover data was used only to run the Geospatial Stream Flow Model for validation purposes. Then 1990, 2000, 2004 and 2010 land use derived maps were used in computing the corresponding streamflows in order to assess the changes on streamflows.

4.1.6 Ground Data for Image Classification

The ground data collected for image classification were geographic coordinates of the different land use/ land cover types and pictures to facilitate posterior interpretation of the field collected data during the supervised image classification process. This was done in the three countries sharing the Incomati basin, where field visits were carried out on previously identified features of land use/ land cover.

4.2 Data Quality Checking and Validation

4.2.1 Filling in Missing Data

To fill in missing data, the linear regression method from the Handbook of Hydrology was used (Salas, 1993). The station with missing data was correlated to the closest neighbouring station with a complete data record for the period of interest. Correlation coefficients between the streamflow data of 5 stations were derived to visualize the level of association between them in order to facilitate the selection of the most related station for use in filling missing data. This was done to fill in missing streamflow data for Ressano Garcia station (E-23) in the Incomati River in Mozambique, and the selected neighbouring station was Komatipoort in South Africa at less than a kilometre away from the first station. The linear regression method applied is described by the following formula:

$$y_t = a + bx_t + \alpha\theta(1-\rho)^{1/2}\sigma_y\varepsilon_t \text{ .... Equation 4. 2}$$

Where:

y_t = dependant variable (runoff from dependent station)

x_t = independent variable (runoff from independent station)

a, b = population parameters of the regression

α = coefficient

θ = 1 when the noise ε_t is added; θ = 0 when ε_t is not added

ρ = population cross-correlation coefficient between y_t *and* x_t

σ_y = population standard deviation of y_t

ε_t = normal uncorrelated variable with mean zero and variance one which is uncorrelated with x_t

The estimation of parameters *a* and *b* is given by:

$$a = \bar{y} - b\bar{x} \text{ .... Equation 4. 3}$$

$$b = rSi(y)/S_i(x) \text{ .... Equation 4. 4}$$

Where:

$\bar{y}$ and $\bar{x}$ *are* the estimated mean of the variable y_t and x_t

Si(y) and *Si(x)* = corresponding estimated standard deviation of y_t and x_t

4.2.2 Data Quality Checking

The quality of the results of any study depends on the quality of the input data used in data analysis. In this study, the main data types for which it was necessary to check for the quality were rainfall (satellite-derived and observed), evapotranspiration (satellite derived) and streamflow (observed) data.

To check the quality of rainfall and evapotranspiration satellite-derived estimates, the sub-basins in which the streamflow gauge stations of interest are located were considered (sub-basins 26, 16, 15, 10 and 19 in Figure 4.1).

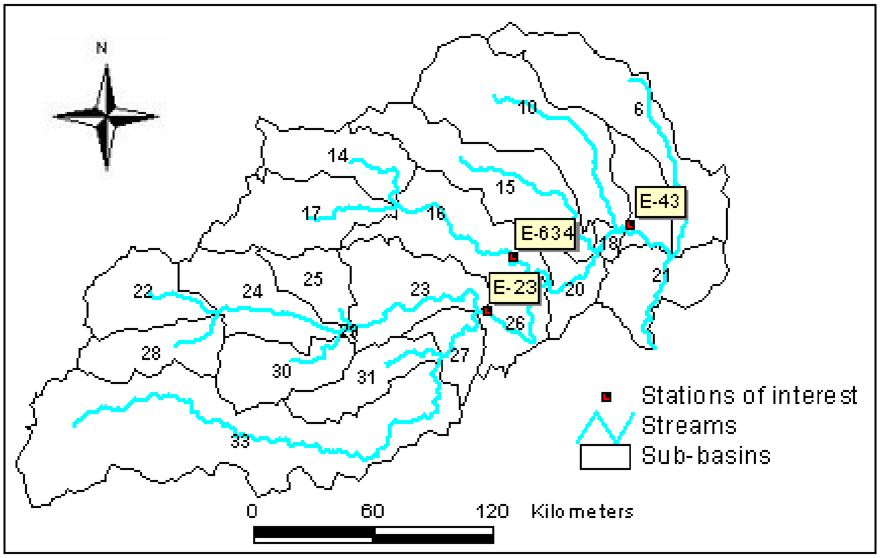

Figure 2.3: Sub-basins considered in rainfall data quality checking

The data quality checking was done through a visual inspection of the rainfall and evapotranspiration time series derived after processing the satellite estimates in the model. This process was done for satellite-derived rainfall and evaporation data from year 2000 to year 2005. Appendix C shows the details of this process.

4.2.3 Data Validation

Data validation is a process that determines the technical usability of the analytical data. In this study the validation was done for satellite-derived rainfall estimates, through a comparison of rainfall time series derived from satellite estimates after processing in the GeoSFM with observed rainfall data of Ressano Garcia (P-586), Magude (P-859) and Manhiça (P-63) in Mozambique. Then a simple regression was done to see how the two types of data were related to each other and at what significance level.

4.3 Data Analysis

4.3.1 Land Use and Land Cover Mapping

The process of mapping land use and land cover change over time began with mapping the 2010 satellite imagery, then looking back into history to map the 2004, 2000 and 1990 satellite imagery. The Landsat images were used due to their relatively good spatial and temporal resolution (30 m and 16 days of spatial and temporal resolution, respectively) and their free availability on the internet. Supervised digital image processing was performed using the *ArcView 3.2 image analysis* extension and ground-based information because satisfactory prior knowledge of the area under study was available and high accurate results were needed. The maximum likelihood algorithm was used to separate the classes defined on the basis of their spectral values across the bands and then the ground based information was used to interpret the derived land use classes.

The definitions of the various land use classes used were as follows and they were based on Anderson *et al.* (1976):

i. Urban and built-up land: comprises areas of intensive use with much of the land covered by structures.

ii. Agricultural land: land used primarily for production of food and fibre. This land use type includes various lower level categories such as cropland and pasture, ornamental horticultural areas; confined feeding operations; and other agricultural land.
iii. Rangeland: land where the potential natural vegetation is predominantly grasses, grass-like plants, shrubs and where herbivores were an important influence in its pre-civilization state. It includes lower level categories such as herbaceous range, shrub and brush rangeland, and mixed rangeland.

iv. Shrubland: typical shrub occurrences are found in those arid and semiarid regions characterized by such xerophytic vegetative types with woody stems and also by the typical desert succulent xerophytes, such as the various forms of Cactus.

v. Forest lands: are areas that typically have a tree-crown areal density of 10% or more, and are stocked with trees capable of producing timber or other wood products, and exert an influence on the climate or water regime. They include 3 lower levels categories namely:

- Deciduous forest: includes all forested areas having a predominance of trees that lose their leaves at the end of the frost-free season or at the beginning of a dry season;
- Evergreen forest: includes all forested areas in which the trees are predominantly those which remain green throughout the year;
- Mixed forest land: includes all forested areas where both evergreen and deciduous trees are growing.

vi. Water bodies: includes all areas that are continuously covered by water. Here are included lower level categories such as streams, canals, lakes, reservoirs, bays and estuaries.

vii. Wetlands: are those areas where the water table is at, near or above the land surface for a significant part of most years. They can include two lower level categories of forested and non-forested wetland.

viii. Barren land: land of limited ability to support life and in which less than one-third of the area has vegetation or other cover. In general, it is an area of thin soil, sand or rocks.

ix. Savannah: a large flat area of land covered with grass, usually with few trees, which is found in hot countries, especially in Africa.

The geographical coordinates representing the different land use classes defined was also used to perform a ground truthing exercise to verify the classification results and possibly improve them. Google Earth images were also used in this process.

a) Land Use Land Cover Reclassification

Geospatial Stream Flow Model uses the Global Land Cover Characterization (GLCC) database (Loveland *et al.,* 2000) derived from 1-km AVHRR data and available in the Lambert Equal-Area Azimuthal projection. The data are used to compute an impervious area grid (MAXCOVER) to account for the presence of water bodies in a sub-basin. GeoSFM includes in its functionality the option to apply user-supplied land use/ land cover data when available. The application of user supplied data is subject to a prior reclassification process, where the derived land cover data sets are reclassified and adjusted to the USGS land cover classification system so that the response coefficients used to compute excess precipitation in Geospatial Stream Flow Model could be associated. Table 4.3 presents the USGS land use/ land cover classes and their respective velocity and Manning's values, used in the reclassification process.

Table 4.3: USGS land use and land cover parameters used in the reclassification

Value	LU_Code	Description	Hyd_A_mean	Hyd_B_mean	Hyd_C_mean	Hyd_D_mean	Velocity	Manning n
0	0	Unclassified	54	70	80	85	0.47300	0.05000
1	100	Urban and Built-Up Land	81	88	91	93	1.97100	0.01200
2	211	Dryland Cropland and Pasture	68	79	86	89	0.59130	0.04000
3	212	Irrigated Cropland and Pasture	62	71	78	81	0.59130	0.04000
5	280	Cropland/Grassland Mosaic	65	75	82	85	0.63925	0.03700
6	290	Cropland/Woodland Mosaic	45	66	77	83	0.33790	0.07000
7	311	Grassland	54	70	80	85	0.67578	0.03500
8	321	Shrubland	45	66	77	83	0.47300	0.05000
10	332	Savanna	57	73	82	86	0.59130	0.04000
11	411	Deciduous Broadleaf Forest	45	66	77	83	0.39420	0.06000
13	421	Evergreen Broadleaf Forest	25	55	70	77	0.23652	0.10000
16	500	Water Bodies	98	98	98	98	0.59130	0.04000
17	620	Herbaceous Wetland	30	58	71	78	0.47300	0.05000
18	610	Wooded Wetland	25	55	70	77	0.23652	0.10000
19	770	Barren or Sparsely Vegetated	68	79	86	89	0.78841	0.03000

b) Assessing the Accuracy of Classification

The level of accuracy of the final classified images was evaluated using the confusion matrix method which compares the classification results to additional ground truth information. The strength of a confusion matrix lies in its ability to identify the nature of the classification errors, as well as their quantities (Nijmeijer, 2001). The computation of the confusion matrix was done using the software ILWIS 3.0.

4.3.2 Trend Analysis of Agricultural Water Abstractions

Use of the Spearman's Rank Correlation Test

A number of correlation test methods such as the Spearman's and Pearson were considered based on their relative simplicity and high validity to hydrological studies as suggested by Altman (1991). The Spearman's Rank Correlation test was selected to investigate the trend in water use by agriculture and forestation in the basin. The Spearman Rank Correlation Test is a non-parametric test which does not make distributional assumptions to the population under investigation. The Spearman's rank coefficient is used as a measure of the linear relationship between two sets of ranked data, that is, it measures how tightly the ranked data clusters around a straight line (Blackwell, 1999). It has been used in many fields and its major difference to other statistical tests is in the fact that no population assumptions are necessary for tests using it and it can perform well if either the data are ordinal, ranked or if it is unreasonable to assume that the variables are normally distributed (Altman, 1991).

In this study two hypotheses were tested regarding changes in agricultural water abstractions in the basin as described below.

Null hypothesis H_0: Rsp = 0 (there is no trend);
Alternate hypothesis, H_a: Rsp < > O (there is a trend.

$$Rsp = 1 - \frac{6 * \sum_{i=1}^{n} Di^2}{n^3 - n}$$ ……………………………………………………………....……Equation 4.5

Where:
Rsp = Spearman's Rank coefficient;
n = total number of data;
D = difference between rankings and it is computed through the following equation:

$$D = K_{xi} - K_{yi}$$ ……………………………………………………………………...…Equation 4.6

i = chronological order number;
K_{xi} = rank of the variable x, which is the chronological order number of the observations;
K_{yi} = rank of the variable y, which is the chronological order number of an observation in the original series.

The Spearman's rank correlation coefficient, like all other correlation coefficient, takes a value between -1 and +1. A positive correlation is one in which the ranks of both variables increase together. A negative correlation is one in which the ranks of one variable increase as the ranks of the other variable decrease. A correlation of -1 or +1 arises if the relationship between the two variables is exactly linear. A correlation close to zero means there is no linear relationship between the ranks.

As the Spearman's Rank Correlation Test only measures the relationship between two data sets, the significance of this relationship was tested using the Rsp values on the Spearman Rank significance table. The interpretation of the results followed the procedure presented in Appendix A.

4.3.3 Trend Analysis of Historical Streamflows Entering in Mozambique

The investigation of changes in streamflows entering in Mozambique was done by testing the hypothesis of occurrence of a trend in the historical flow data through the Spearman's Rank

Correlation Test described in the section 4.3.2. Two border stations located in the Incomati and Sabie Rivers were analyzed for trend (Ressano Garcia E-23 and Corumana dam E-630), as shown in Figure 4.4.

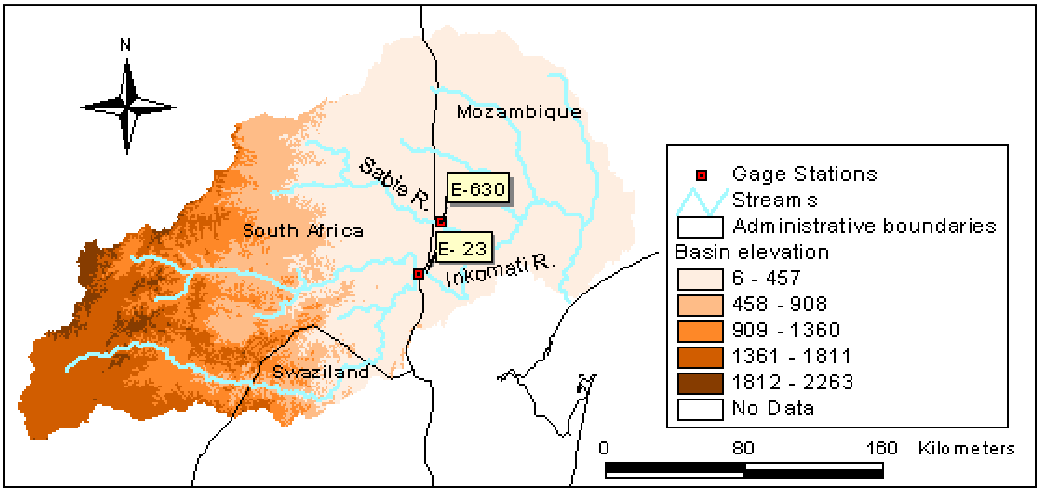

Figure 4.4: Location of the flow stations used in trend analysis

4.3.4 Modelling the Impacts of Land Use in Streamflow

Use of Geospatial Stream Flow Model

To model the effects of land use changes in streamflows, the land use maps obtained from 1990, 2000, 2004 and 2010 classified images were input into GeoSFM as user supplied land use maps. The model was run using rainfall and evapotranspiration data from year 2000 to 2004 for all the land use maps in order to isolate their effect in the analysis. T-test was performed to assess the statistical significance of streamflow changes in the different sub-basins because it is considered appropriate whenever one want to compare the means of two groups.

a) Compute Terrain Analysis for Flow Routing

The analysis of topographic data for hydrologic modelling applications relies on the simple principle that water flows in the direction of steepest descent. Hence, by comparing the elevation of a given cell with that of the eight surrounding cells, it is possible to determine which direction the incident drops of water would flow. Flow direction in GeoSFM is assigned using the eight direction pour point model (Jenson and Dominque, 1988), in which each grid cell is assigned one of eight compass directions depending on which of its eight neighbouring cells its discharge flows to. The 8-direction flow algorithms used by GeoSFM to assign the direction of flow to each cell are: 1 (East), 2 (Southeast), 4 (South), 8 (Southwest), 16 (West), 32 (Northwest), 32 (North) and 128 (Northeast) (Figure 4.5).

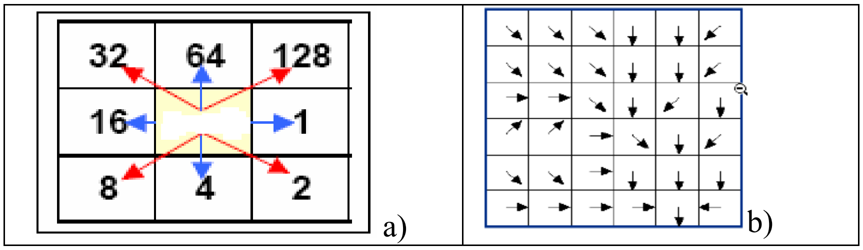

Figure 4.5: Principle for creating flow direction grid (a) and example of flow direction representation (b). Source: Adapted from ILWIS software (Nijmeijer, 2001).

b) Basin Characterization Routine

The basin characterization routine summarizes the elevation derivatives, soil and land cover parameters over each sub-basin and exports the results into ASCII files formatted to GeoSFM specifications. For any river basin application, the basin characterization is only performed once during the model creation phase, and the output files are stored for access by subsequent simulation routines.

c) Unit Hydrograph Generation Routine

GeoSFM contains a routine where a unit hydrograph is developed to simulate the typical response of the catchment to a uniformly distributed water input event. The unit hydrograph is developed for each catchment during the model pre-processing phase for posterior use (Asante *et al.*, 2008). In the same routine, GeoSFM computes the uniform overland velocity for each catchment based on the mean slope of the catchment and dominant land cover type present. The distance along the flow path from each grid cell in the catchment to the catchment outlet is also computed. The travel time from each grid cell to the catchment outlet is also computed as shown in the equation 4.7 (Entenman, 2005; United States Geological Survey, 2001).

$$t_i = \frac{l_i}{v_i} \quad \text{..........Equation 4.7}$$

Where:

t_i - travel time from a given grid cell to the basin outlet

l_i - flow length from a given grid cell to the basin outlet

v_i - average overland velocity for the basin

At the end of the process the distribution of discharge at the catchment outlet is given by the probability density function (PDF) of travel times in the catchment.

d) Generation of Rainfall and Evaporation Files

GeoSFM contains algorithms for computing mean areal rainfall (MAR) and mean areal evapotranspiration (MAE) values for each catchment from satellite-derived rainfall and evapotranspiration estimates after converting them to grids through the image analyst extension in ArcView. The generation of rainfall and evapotranspiration time series in ASCII format is the final step before the initiation of hydrologic model runs.

e) Soil Moisture Accounting Module

As a continuous simulation model, GeoSFM contains routines for computing runoff and soil moisture conditions daily. The two options provided for performing this accounting in GeoSFM are the Linear Soil Moisture Accounting (LSMA) and the Nonlinear Soil Moisture Accounting (NSMA) modules (Asante *et al.,* 2008). Irrespective of the choice of soil moisture accounting model, GeoSFM generates a series of ASCII files containing the surface interflow, baseflow, and percolation fluxes as well as the soil moisture storage as shown in the Figure 4.6.

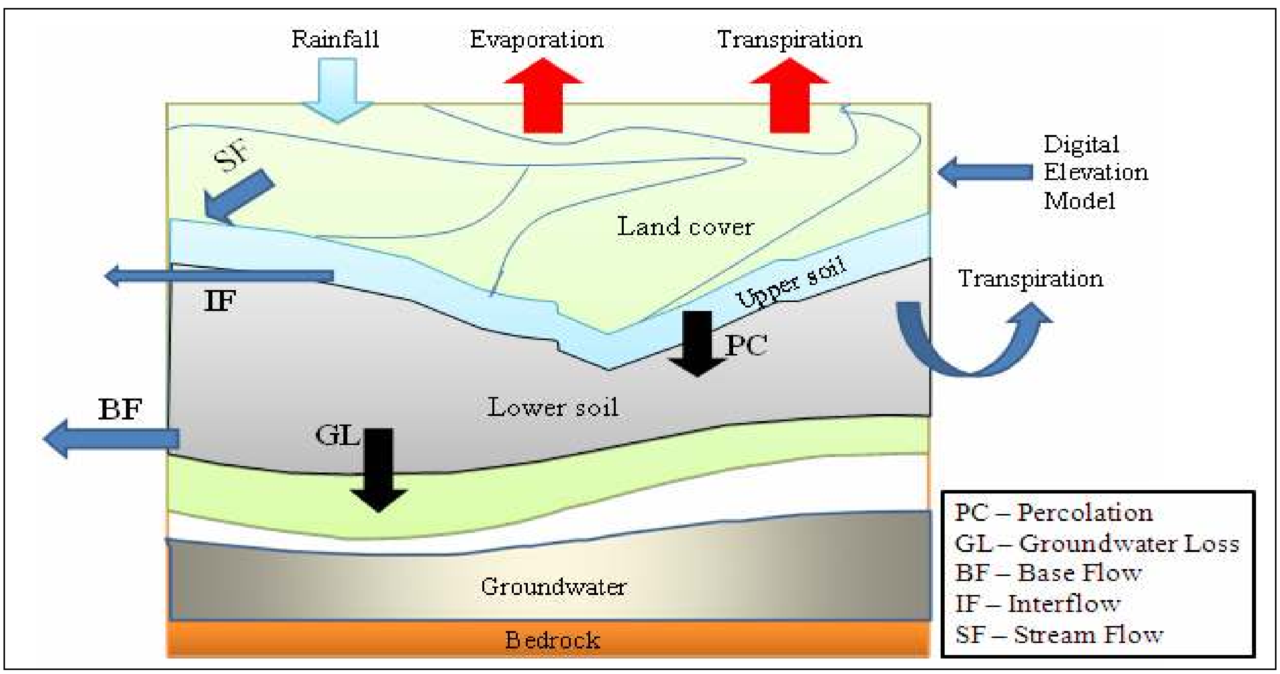

Figure 4.6: Schematization of the conceptual water balance model applied in GeoSFM. Source: Adapted from United States Geological Survey (2001)

Mathematically the processes above are represented by the general water balance equation as shown below:

$$\Delta S = P - ET - D - R \quad \text{.......Equation 4.8}$$

Where:

ΔS = Change in soil water content (mm)

ET = evapotranspiration = soil evaporation and transpiration (mm)

D = Drainage or loss (mm)

P = Precipitation (mm)

R = Recharge to the groundwater system (mm)

f) Streamflows

After computing the water balance, GeoSFM compute the streamflow using many routing methods. In this study the diffusion analogue was used, due to its ability of going beyond the lag routing by accounting for both flow advection (using flow time or celerity) and attenuation (using a flow dispersion coefficient) (Asante *et al.,* 2008). Mathematically, the diffusion analogue equation can be expressed as shown below (Equation 4.7).

$$Q(t) = I(t_o).(\frac{x}{\sqrt{4 \cdot \pi \cdot D(t-t_o)^3}}) \cdot \exp\left[-(\frac{(v \cdot (t-t_o)-x)^2}{4 \cdot D(t-t_o)})\right] \quad \text{.......Equation 4.9}$$

Where:

D = Dispersion coefficient (m^2/s)

v = Flow celerity (m/s)

x = Length of the river reach (m)

t_o = Time of the input event (s)

t = Present time (s)

$Q(t)$ = Discharge at the downstream end of the river reach (m^3/s)

$I(t_o)$ = Inflow at the upstream end of the river reach (m^3/s)

g) Calibration

GeoSFM includes an automatic calibration method intended to improve the application of the model. Due to uncertainties in the input and output data sets, model structure error, and the quantity or quality of data, it is difficult to determine a best set of model parameters (Duan *et al.,* 1992). Thus, the model includes a sensitivity analysis with the purpose of identifying the most sensitive input parameters that influence the model outputs. This analysis is performed prior to calibration, which basically adjusts the identified sensitive parameters to match as much as possible to the real world system. In this study, four parameters were identified as the most sensitive, namely *SoilWhc, Depth, Ks and CurveNum.* In the calibration process after selecting the parameters the maximum number of runs was defined and in this study 1600 were found as ideal based on the results they gave. The best set of the model parameters obtained after calibration was used to run the model for the land use scenarios defined in 4.3.1.

h) Model Verification

The verification of the model performance was done by first comparing the observed streamflows and modelled ones. This process was done before and after model calibration and a regression (R^2) was done to see how the two compared streamflows matched. In addition, the Root-Mean-Square-Error (RMSE) was evaluated using the equation 4.10 from Walford (1994) to verify the results produced by the model after calibration process. For model verification there were used the Ressano Garcia (E-23) and Magude (E-43) gauge station because the data of both stations was relatively consistent with few gaps.

$$RMSE_m = \sqrt{\frac{1}{N}\sum_{i=0}^{N}\left[Fm(Z_i) - fm(Z_i)\right]^2} \quad \text{……………………………………..….Equation 4.10}$$

Where:

N = Total number of observations
F_m = Observed data
f_m = Forecasted data

The RMSE is thus the distance, on average, of a data point from the fitted line, measured along a vertical line and it has the same units as the quantity plotted on the vertical axis. In this study the RMSE was done for E-23 and E-43.

4.3.5 Investigation of Streamflows at Key Gauge Stations for Flow Monitoring According to IIMA

In order to assess whether the changes in streamflows entering Mozambique were not a consequence of upstream dam operation procedures and rainfall dynamics, a thorough study of streamflows at key gauge stations for flow monitoring as defined by the IncoMaputo Interim Agreement (IIMA) was done. The analysis compared the observed and the IIMA stipulated flows at key stations. The analysis was done for both daily and annual flows of the period 2002/03 to 2009/10 as IIMA entered into force in 2002. Flow duration curves were done to determine the percentage of time for which the IIMA stipulated flows were equalled or exceeded at specific stations. This was done to verify the level of compliance with the Agreement by the three member States. Total annual rainfall figures of each station were included in the analysis in order to clearly visualise their influence on the observed river flows.

Due to data unavailability constraints the analyses were done for 3 stations, namely Lower Sabie (X3H015), Tenbosh (X2H016) and Ressano Garcia (E-23).

CHAPTER 5

5.0 RESULTS AND DISCUSSIONS

This chapter presents the study results and discussions in basically four sub-sections: Changes in land use and agricultural water abstraction, changes in river flows at key gauge stations, modelling the impacts of land use changes on river flow and analysis of streamflows at key gauge stations for flow monitoring as stipulated by the IncoMaputo Interim Agreement.

5.1 Changes in Land Use and Agricultural Water Abstraction

5.1.1 Changes in Land Use

a) Land Use Classification

From the supervised imagery classification the following land use/ land cover classes were obtained: residential areas, agricultural areas, sugarcane plantations, shrubland, grassland, savannah, deciduous forest, evergreen forest and water bodies. In the reclassification process the obtained land use and land cover types were adjusted to USGS classification system and the results are shown in the Table 5.1.

Table 5.1: Reclassification and association of derived land use/land cover classes.

S. No	Incomati landuse land cover classification	Value	USGS Land use code	USGS Description	Mean curve numbers for hydrologic soil groups				
					A	B	C	D	Velocity
1	Residential areas	1	100	Urban and Built-Up Land	81	88	91	93	1.97100
2	Agricultural area	2	211	Dry land Cropland and Pasture	68	79	86	89	0.59130
3	Sugar cane plantations	3	212	Irrigated Cropland and Pasture	62	71	78	81	0.59130
4	Grassland	7	311	Grassland	54	70	80	85	0.67578
5	Shrubland	8	321	Shrubland	45	66	77	83	0.47300
6	Savannah	10	332	Savannah	57	73	82	86	0.59130
7	Deciduous Forest	11	411	Deciduous Broadleaf Forest	45	66	77	83	0.39420
8	Forest	13	421	Evergreen Broadleaf Forest	25	55	70	77	0.23652
9	Water	16	500	Water Bodies	98	98	98	98	0.59130

b) Mapping the Changes in Land use/ Land Cover

Based on the analyses of Landsat TM images of the Incomati River basin for the years 1990, 2000, 2004 and 2010, land cover thematic maps were obtained (Figure 5.1). The changes in the area of the basin covered by each land use/ land cover type are shown in Table 5.2.

Between 1990 and 2010 there has been a decrease in evergreen forests of 46%. The reduction can be attributed to clearing of forests for agriculture, timber and settlement. Irrigated cropland and pasture land have increased by 310%.

The rangelands (grassland and savannah) have decreased by 2% and 32%, respectively. Shrubland has increased by 1056% and this can be attributed to the expansion of areas of commercial plantation which are considered to be currently one of the major land use types in the basin according to TPTC (2010). Water bodies have reduced by 37% and this may be due to the decrease in the total water surfaces such as wetlands and natural lakes in the basin as a result of many factors among which the human induced ones are of high consideration.

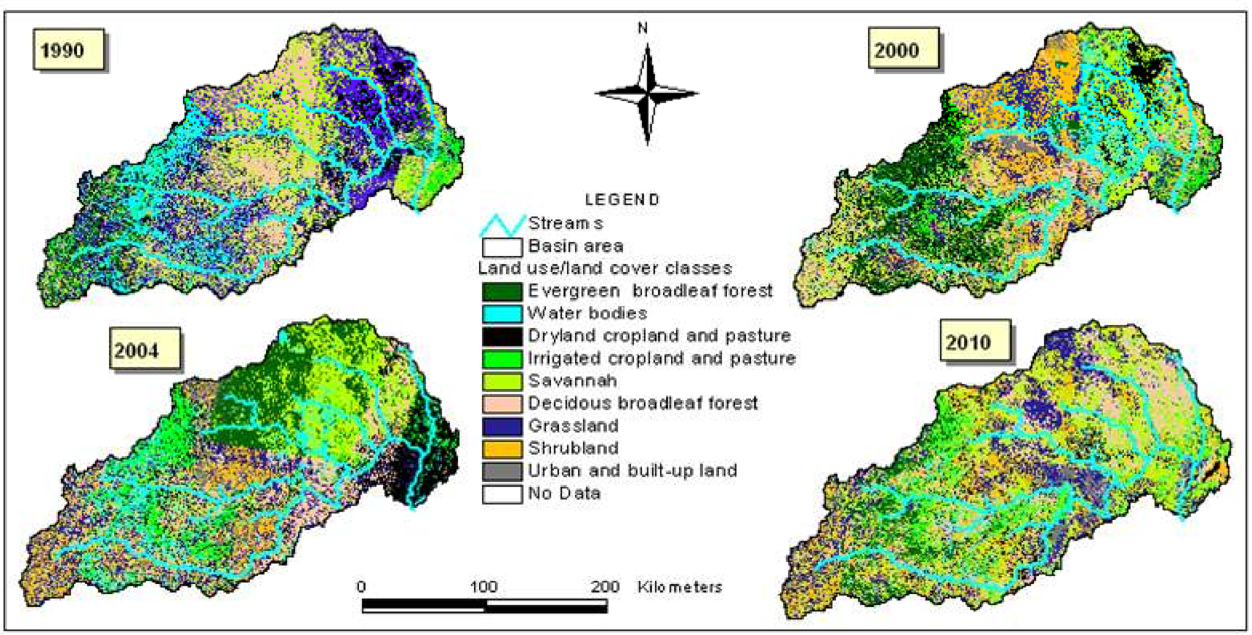

Figure 5.1: Land use/ land cover maps for 1990, 2000, 2004 and 2010 for the Incomati basin

Table 5.2: Land use/ land cover changes statistics

Class No.	Class Name	Number of Pixels ($*10^6$)				% of change (1990 - 2010)
		1990	2000	2004	2010	
1	Evergreen broadleaf forest	2.98	1.04	7.02	1.62	-46
2	Water bodies	4.51	0.92	3.80	2.86	-37
3	Dryland cropland and pasture	6.95	1.65	5.52	4.76	-32
4	Irrigated cropland and pasture	2.21	1.07	4.20	9.05	310
5	Savannah	11.40	2.50	8.37	11.18	-2
6	Deciduous broadleaf forest	8.34	1.79	6.76	8.03	-4
7	Grassland	10.82	2.08	6.59	7.34	-32
8	Shrubland	0.30	2.14	5.50	3.45	1056
9	Urban and built-up land	0.73	1.81	2.54	2.79	285

c) Accuracy of the Land Use/ Land Cover Classification Process

The verification of the accuracy of the derived land use maps was performed only for the 2010 land use/ land cover classification result because it is the year whose data from field work was available. The overall accuracy of the classified land use/ land cover map was 71%, which means that from the total number of pixels classified, 71% were correctly classified (Table 5.3). The results suggested that classes such as savannah, and urban and built-up land were difficult to classify and hence the lower accuracies of 37% and 46%, respectively. This can be associated mainly with the quality of the Landsat images used, which in some cases gave the same reflectance values for features that were different on the ground.

Table 5.3: Confusion matrix for the 2010 land use/ land cover derived map

		CLASSIFICATION RESULTS									TOTALS	Accuracy (%)
		Deciduous broadleaf forest	Dryland cropland and pasture	Evergreen broadleaf forest	Grassland	Irrigated cropland	Savannah	Shrubland	Urban and built-up land	Water bodies		
GROUND THRUTHING	Deciduous broadleaf forest	19	0	0	3	1	0	0	2	0	25	76.00
	Dryland cropland and pasture	0	7	0	0	0	0	0	0	0	7	100.00
	Evergreen broadleaf forest	1	0	22	0	3	2	2	0	0	30	73.33
	Grassland	0	3	0	17	3	1	2	0	0	26	65.38
	Irrigated cropland and pasture	0	0	0	0	23	1	1	0	0	25	92.00
	Savannah	2	1	0	3	0	7	3	3	0	19	36.84
	Shrubland	1	1	0	0	0	0	15	0	1	18	83.33
	Urban and built-up land	2	6	0	1	0	2	3	12	0	26	46.15
	Water bodies	1	1	0	0	0	0	0	0	22	24	91.67
	TOTALS	26	19	22	24	30	13	26	17	23	200	
	RELIABILITY (%)	73.08	36.84	100.00	70.83	76.67	53.85	57.69	70.59	95.65		
Avarage accuracy												**73.86**
Overall accuracy												**70.58**
Overall reliability												**72.00**

5.1.2 Changes in Agricultural Water Abstractions

From the calculation of agricultural water abstraction the values presented in the Figure 5.2 were found. The graph shows that the water abstractions have been increasing even before 1990, but the rate of change has increased from 1990 to 2010.

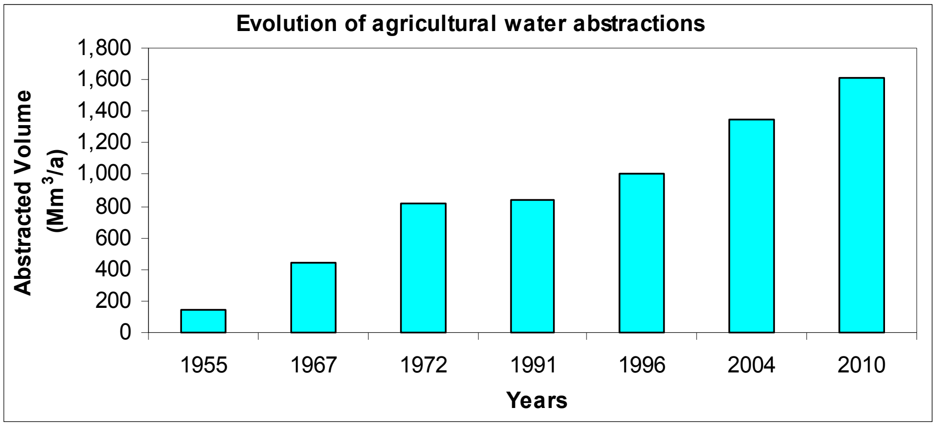

Figure 5.2: Evolution of agricultural water abstraction in the Incomati basin

From the Spearman's Rank Correlation Test, a perfect trend in agricultural water abstraction was found, i.e, Rsp=1. A perfect trend refers to cases where the Spearman's Rank Correlation Coefficient (*Rsp*) is equal to -1 or +1. The coefficient was positive and that means that there has been an increase in agricultural water abstraction in the basin for a long time. The significance level test resulted in 1%, which means that there is a confidence level of 99% that the changes have not occurred by chance (Figure 5.3).

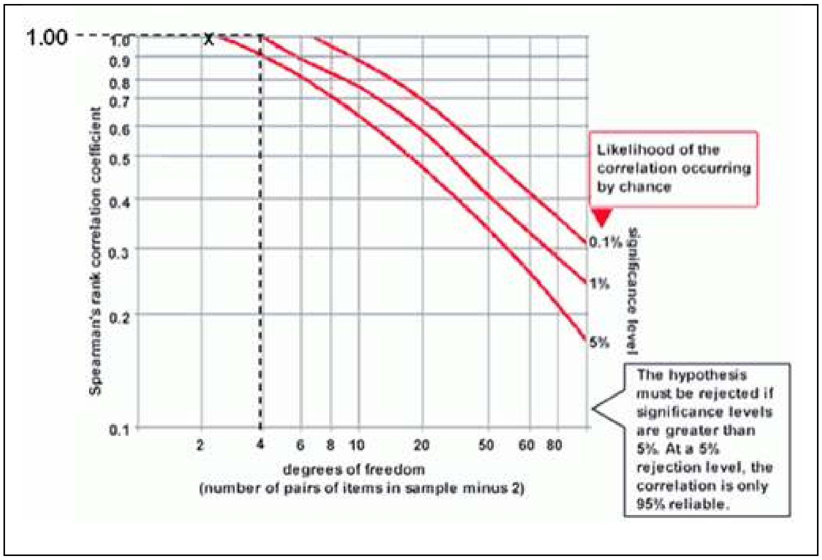

Figure 5.3: Spearman's significance level and level of freedom of the change in historical agricultural water abstractions in the Incomati River basin

Figure 5.2 shows that in the period between 1955 and 1967, agricultural water use in the Incomati basin was modest and no major dams existed, though developments were happening quickly and the first ideas for further water development had become clear (Vaz and van der Zaag, 2003). This justifies the relatively low agricultural water use in the basin for the period 1955-1967. In the period 1972–1991, agricultural water use increased in comparison with the previous period because between the years 1972 and 1981, four relatively small dams were built in the basin (each smaller than 15 Mm^3), three on the Crocodile and one on the Sabie, all in South African territory (Vaz and van der Zaag, 2003). From 1996 to 2010 agricultural water use experienced its highest increase in the basin and this can be attributed to an increase in agricultural developments, mainly at the South African side of the basin, motivated by an increased assurance in water supply. The increased assurance in water supply was brought by major developments in water storage infrastructure that has taken place in the basin since 1990 (construction of the Maguga Dam with 332 Mm^3 capacity in Swaziland, Driekoppies and Injaka Dams with 251 Mm^3 and 120 Mm^3 capacities respectively in South Africa) (TPTC, 2010).

5.1.3 Other Water Uses: Domestic, Industrial and Mining

Domestic and industrial water uses have increased in the basin with an average of 2 Mm^3/a and 0.7 Mm^3/a, respectively (Figure 5.4).

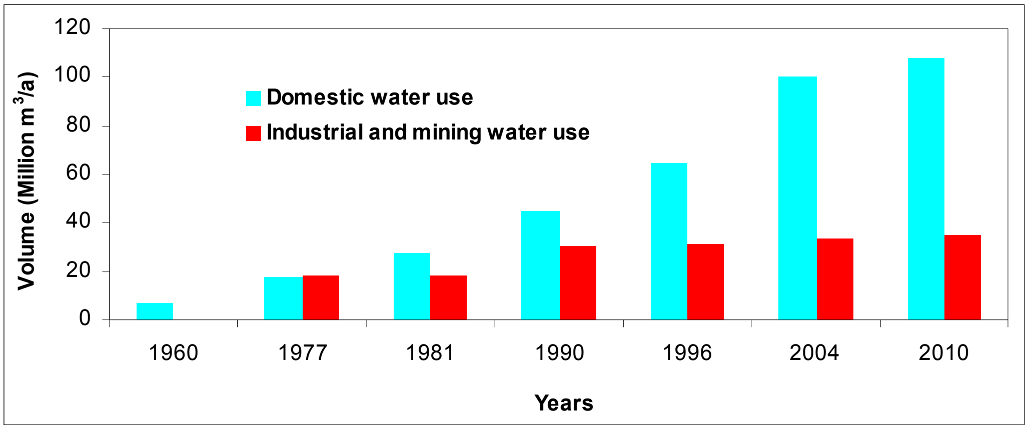

Figure 5.4: Historical growth of other water uses in the Incomati basin

From Figure 5.4, in the case of domestic water use, the increases can be attributed to population growth related to establishment of new towns in the basin mainly on the South African side. In the case of industrial and mining water use, the expansion of industrial plants led mainly by the sugar cane sector can be the major contributor. When looking specifically at the period from 1990 up to 2010, it can be seen that in the case of industries and mining there has been a relatively slow growth in water use when compared to the period before 1990. This can be explained by either lack of new industries during the last two decades or improvement of production technologies to less water consumptive ones in South Africa and Mozambique.

5.2 Changes in River Flows at Key Gauge Stations

5.2.1 Trend Analysis of River Flow at Ressano Garcia (E-23) and Corumana Dam (E-630)

From the Spearman's Rank Correlation Test, it was found that Spearman's Rank Coefficients had values of $Rsp= -0.57$ for Ressano Garcia (E-23) and $Rsp=0.40$ for Corumana dam (E-630). This suggests that the null hypothesis of non-existence of trend is rejected. On the other hand, in terms of significance, it was found that Ressano Garcia had a significance level above 0.1% which means that the probability of the observed trend being a chance event is low. In other words we can be 99.9% confident that the trend has not occurred by chance (Figure 5.5). For Corumana dam, a significance level below 5% was found and that suggests that the change occurred by chance. In this case the null hypothesis is accepted, meaning that there have not been significant flow changes at E-630.

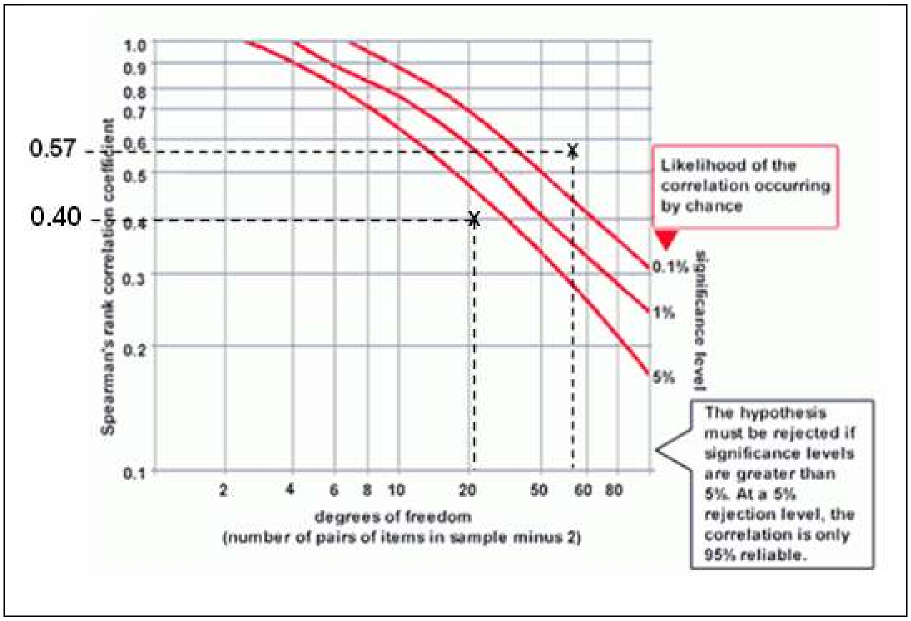

Figure 5.5: Spearman's significance and level of freedom of the change in stream flows at E-23 and E-630

Figure 5.6 shows the behaviour of flows at Ressano Garcia. The long term trend indicates a decrease in flows looking at the period from 1952 to the year 2010. Between the years 1952/1953 and 1989/1990 the average annual flow was 2456 Mm^3/a, and between 1990/1991 and 2009/2010 the average flow was 1175 Mm^3/a. This shows an average decrease of 52% in the flows between the two periods. In addition, it can be seen that for the period 1990-2010 the frequency of low flows has increased.

The existing rainfall data for Ressano Garcia shows a pattern nearly related to the one for flows, although there was not a match between the peak flows and peak rainfall. This shows a reduced influence of the local rainfall in flows in this station and it can be attributed to the fact that the flows passing in this station being a direct consequence of upstream climate and dam operation at South Africa and Swaziland.

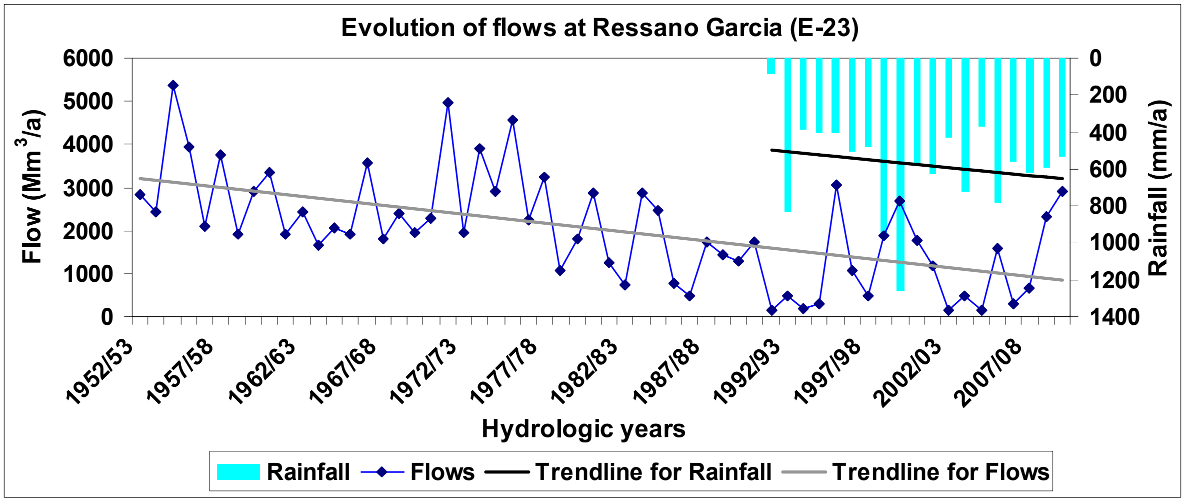

Figure 5.6: Flows dynamics at Ressano Garcia (E-23)

5.2.2 Flow Dynamics at Upstream Catchments of the Basin

a) Komati Catchment

The Komati is the major catchment of the Incomati basin and it is shared by South Africa and Swaziland. Figure 5.7 shows the annual flow dynamics observed in the main gauge stations of the catchment starting from different periods according to the data available. Tonga (X1H003), which is downstream of all the other stations of the Komati, shows a systematic reduction of flows with time, and an increase of frequency of low annual flows (less than 200 Mm^3/a) since 1990. This situation is similar for Hoogenoeg station (X1H001) which is upstream of the catchment. Stations at Mananga and downstream of Vygeboom dam show a stable flow cycle which can be attributed to the fact that they are immediately downstream of dams (Maguga and Vygeboom dams respectively) where the flows are a direct result of the releases done in accordance to the operational rules in use for the dams.

The observed annual rainfall shows a similar trend as the flow pattern, with the peak flow at Tonga coinciding with the maximum rainfall for the period of analysis. Finally, it can be concluded that the observed streamflow behaviour at this catchment was largely influenced by the rainfall pattern.

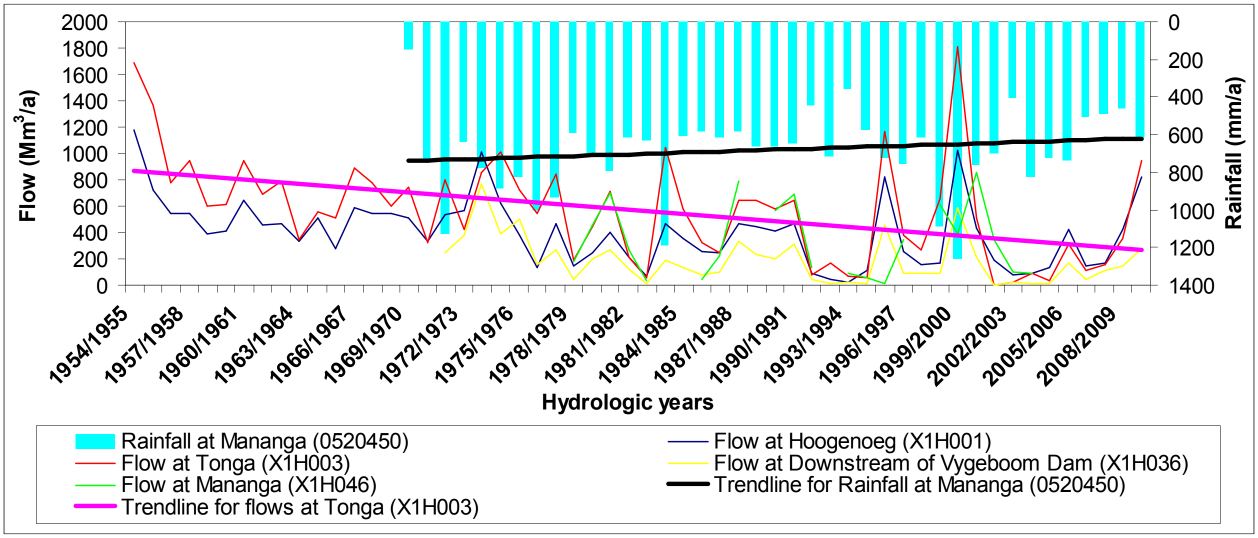

Figure 5.7: Flow dynamics in the Komati Catchment

b) Sabie Catchment

This catchment is part of the Incomati and it is shared by South Africa and Mozambique. The catchment drains to the Corumana dam in Mozambique. Data series for this catchment are relatively short because the gauge stations are new (Figure 5.8). From existing data, it can be seen that the flows at the main stations of the catchment show a stable behaviour throughout the time. In the same figure, rainfall pattern is also presented for the same period as the flows and it can be seen that there is an agreement between the two for most of the time. However, there have been some years in which this pattern was not observed at all (1999/2000, 2001/2002, and 2004/2005) and this can be attributed to the effect of other factors. In regard to land use dynamics in this catchment, little is expected as major area of the catchment is under the Kruger Park.

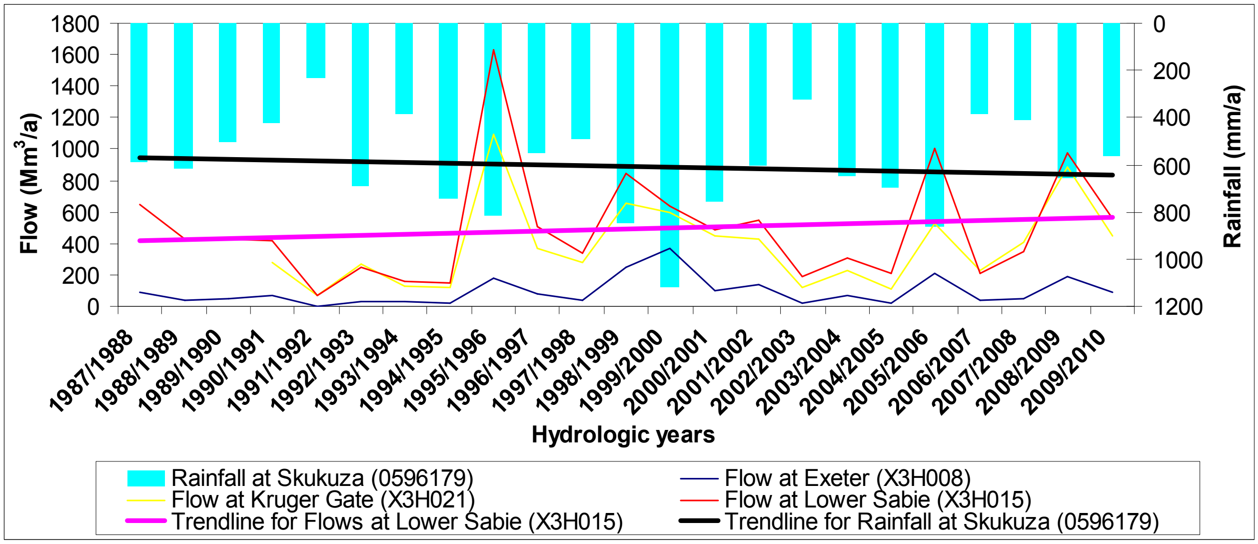

Figure 5.8: Flow dynamics in the Sabie Catchment

c) Crocodile Catchment

It is the second largest catchment of the Incomati basin after Komati and it is located entirely in South Africa. The flows at the main stations of the catchment show generally a stable situation since the year 1955, which can be partly attributed to the rainfall pattern observed which followed the same pattern. In addition, the observed flow behaviour can be attributed to the fact that the catchment is still in development and the existing major water users are new. However, from 1990 the frequency of low annual flows has increased compared to the period before (Figure 5.9).

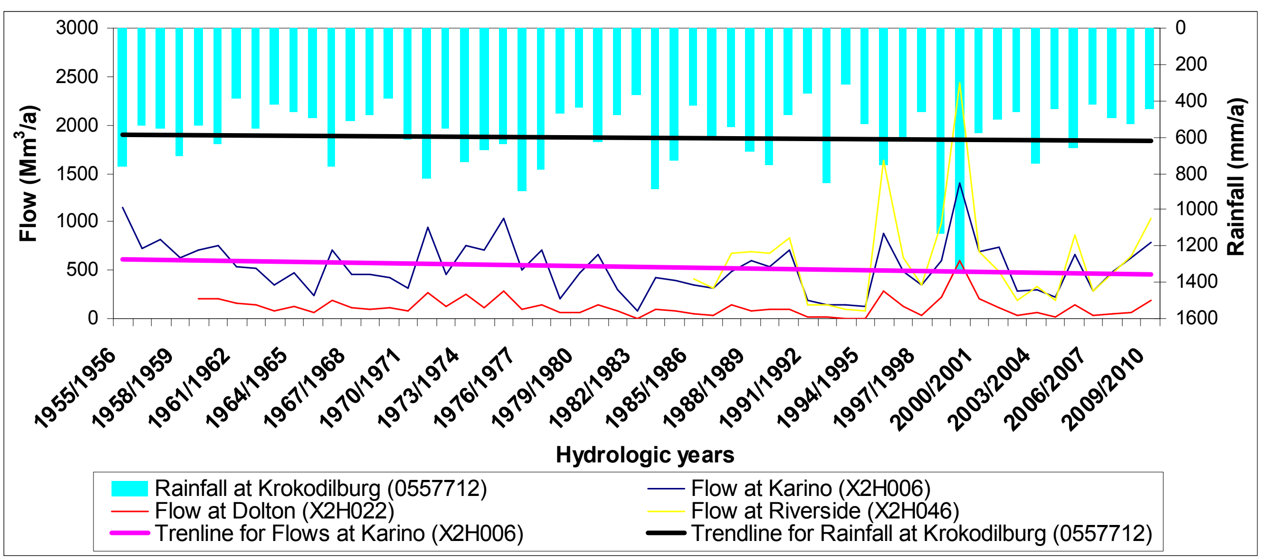

Figure 5.9: Flow dynamics in the Crocodile Catchment

5.3 Modelling the Impacts of Land Use Changes on River Flow

This subsection presents the modelling findings which are basically structured in the following sequence: data validation, model verification (only for Ressano Garcia (E-23) and Magude (E-43) because of time constraints), actual modelling of land use changes and statistical analysis of the forecasted streamflows.

5.3.1 Data Validation

a) Comparison between Observed and Forecasted Rainfall

Figure 5.10 shows the comparison between observed and satellite-derived rainfall (forecasted) for January 2000 at Ressano Garcia (P-856). It can be seen that there is in general an agreement between the two types of rainfall data, what is even much more prominent in days where there is no rainfall. However, it can be seen that in some days there have been over and underestimation on rainfall and this can be associated to many reasons, among which could be: the recording errors by the gauge readers, evaporation and wind influences.

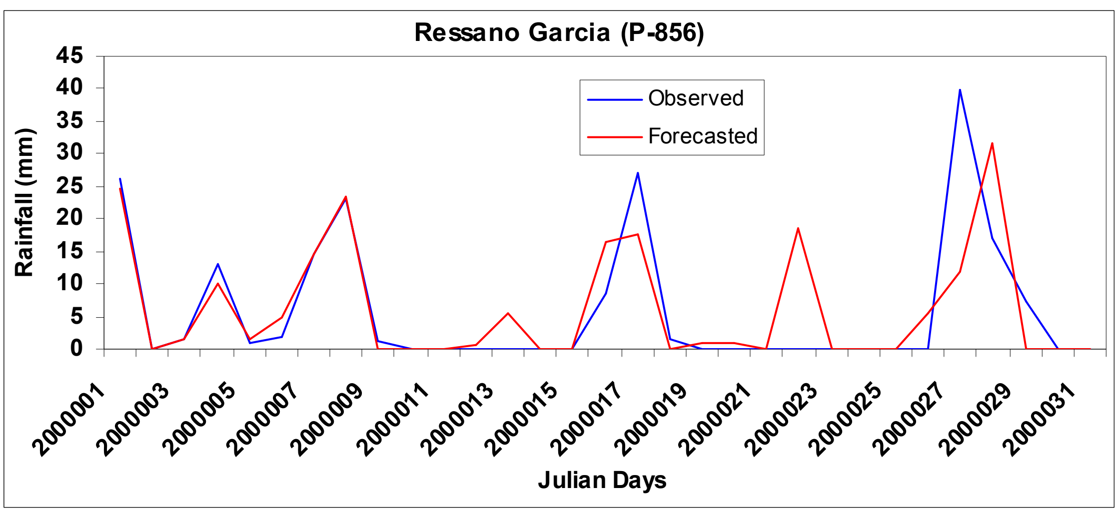

Figure 5.10: Comparison between observed and forecasted rainfall at Ressano Garcia

Figure 5.10 together with Figure 5.11, shows the relationship between the observed and forecasted rainfall. It can be seen that forecasted rainfall can be used as data in modelling or another kind of exercises with a good degree of confidence, as shown below by the significantly high regression coefficients obtained for Manhiça (P-63) and Magude (P-589) (R^2 = 0.76 for Manhiça and R^2 =0.93 for Magude).

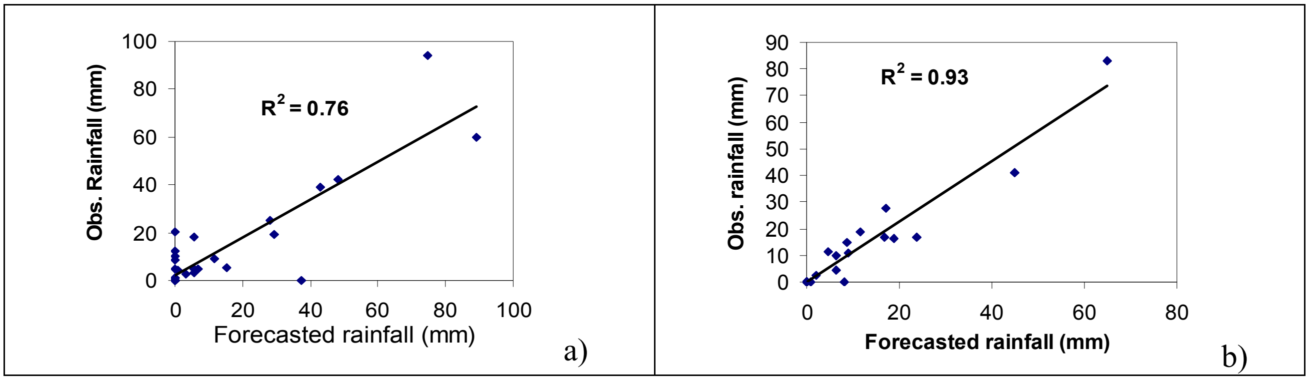

Figure 5.11: Regression between observed and forecasted rainfall data at Manhiça (a) and Magude (b) for 2000

5.3.2 Model Testing

a) Comparison between Observed and Forecasted Streamflows before Model Calibration

I. Ressano Garcia (E-23)

The comparison between the observed and forecasted streamflows showed an agreement between the two, especially in trend. At Ressano Garcia for both peaks observed on the Julian days 2001003 and 2001347 of 278 m^3/s and 317 m^3/s respectively, the model produced the corresponding peaks which varied in magnitude but occurred in the same days. For low flows the model results gave a better approximation with the actual situation on the ground (Figure 5.12).

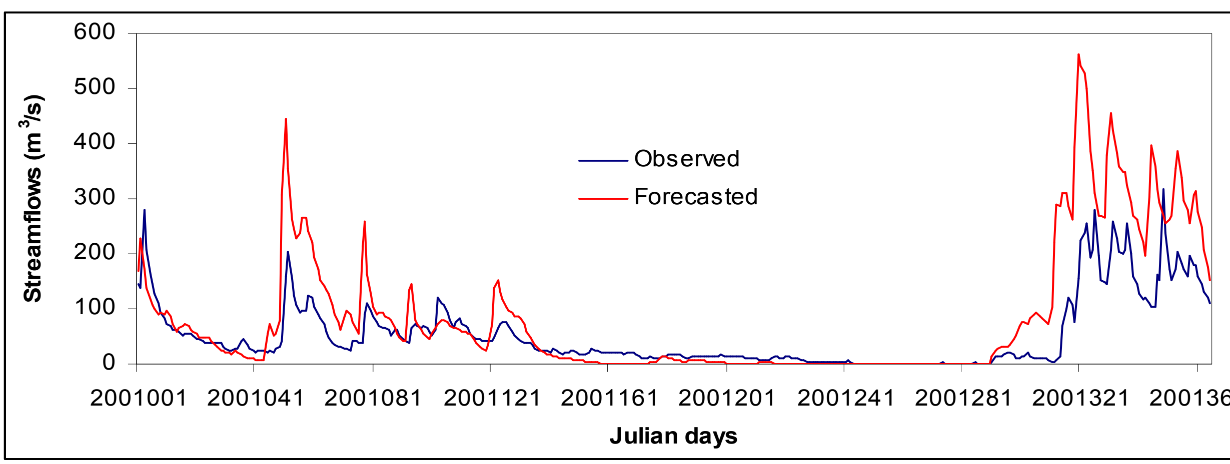

Figure 5.12: Comparison between observed and forecasted streamflows at Ressano Garcia before calibration (E-23)

II. Magude (E-43)

At this station the model outputs had a good approximation with the observed situation even before calibration. The peak flows of both forecasted and observed daily streamflows occurred in the same period, between 2001053 and 2001056 for the first peak, and between 2001325 and 2001338 for the second peak flow. For low flows the model results gave a better approximation with the actual situation on the ground (Figure 5.13).

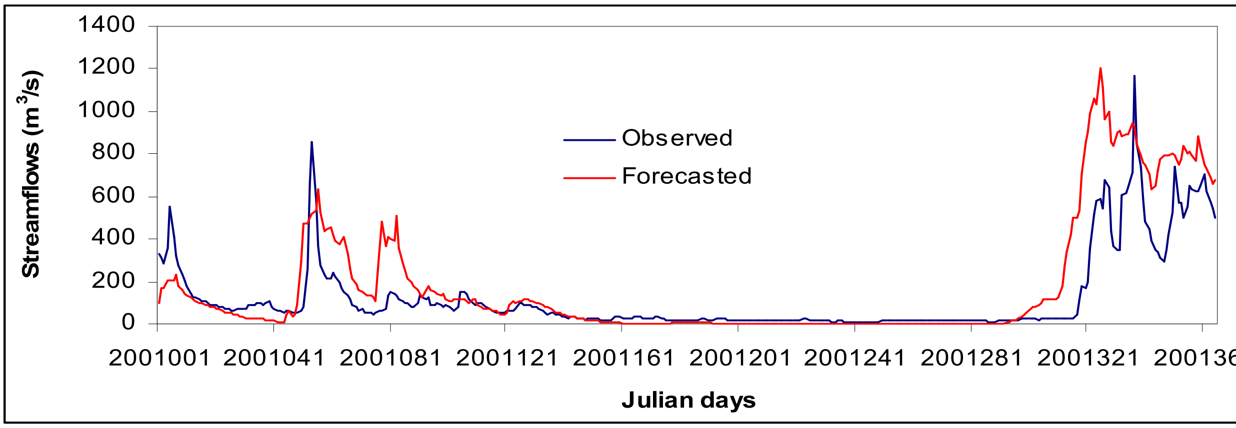

Figure 5.13: Comparison between observed and forecasted streamflows at Magude before calibration (E-43)

b) Comparison between Observed and Forecasted Streamflows after Model Calibration

I. Ressano Garcia (E-23)

After model calibration the peak flows of forecasted streamflows adjusted better to the observed ones. A much better fit was achieved for low flows, where for almost all the time the observed streamflows were almost equal to the forecasted flows (Figure 5.14).

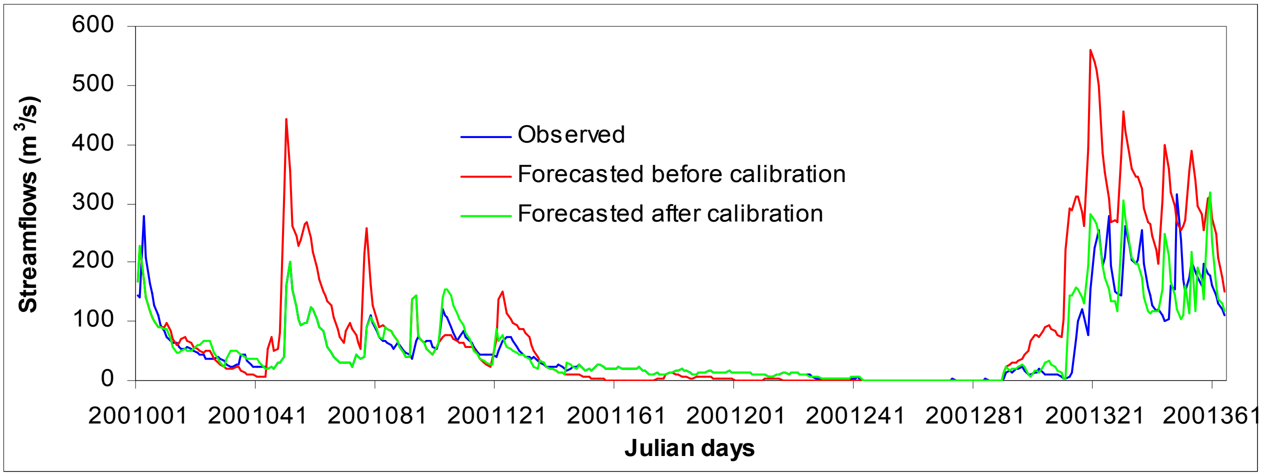

Figure 5.14: Comparison between observed and forecasted stream flows after model calibration at E-23

II. Magude (E-43)

After model calibration the peak flows of both observed and forecasted became of approximately the same magnitude, and occurred on the same dates (Julian days 2001054 and 2001337). The low flows have adjusted better in magnitude than before calibration and in terms of the period of occurrence they were observed in the same time as before calibration (Figure 5.15).

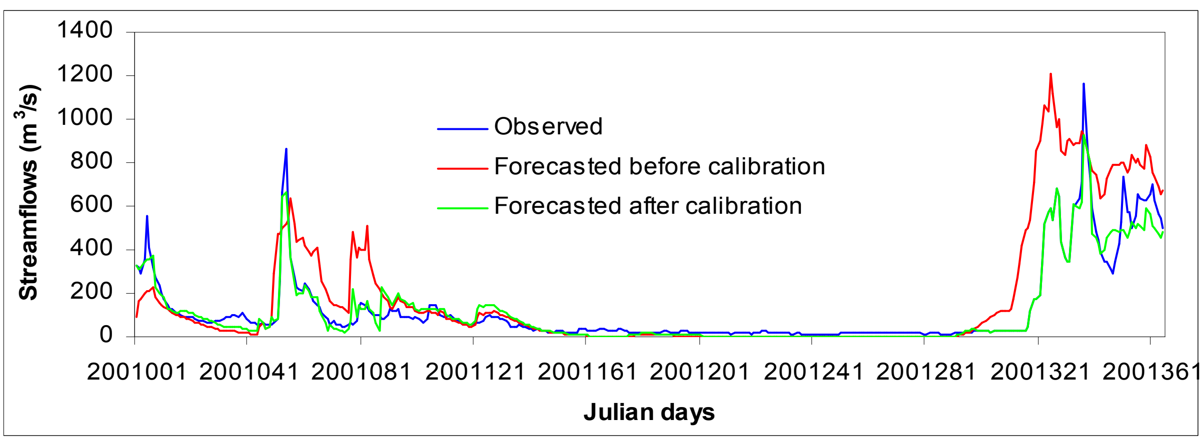

Figure 5.15: Comparison between observed and forecasted stream flows after model calibration at E-43

5.3.3 Model Verification and Performance

a) Statistical Significance

Figure 5.16 shows positive, strong and significant relationships at $p<0.05$ between the forecasted and observed streamflows at Ressano Garcia (E-23) and at Magude (E-43), before and after model calibration, for N=365. However, through the R^2 values, it can be seen that the calibration process have improved the fitness between the observed and forecasted streamflows for both stations (Before calibration: Ressano Garcia – R^2=0.73, Magude –R^2=0.75; after calibration: Ressano Garcia – R^2=0.78, Magude – R^2=0.94).

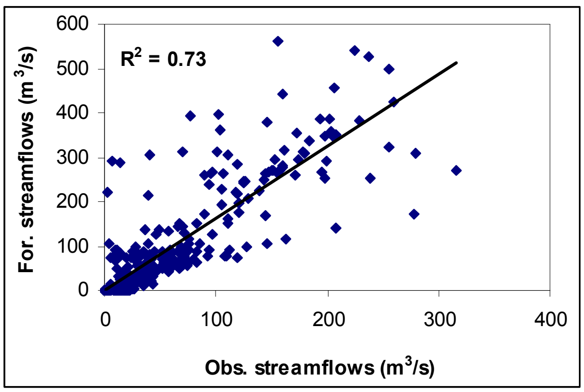

a) E-23: Before model calibration

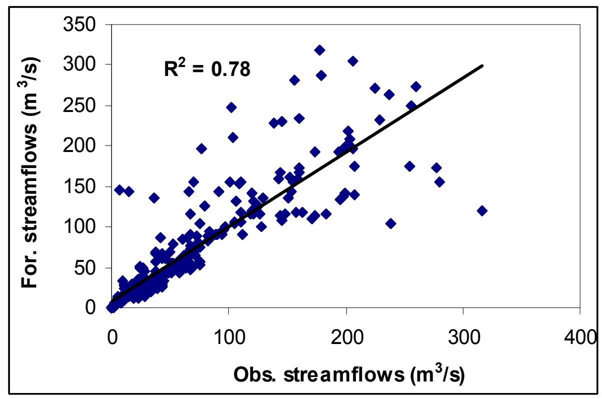

b) E-23: After model calibration

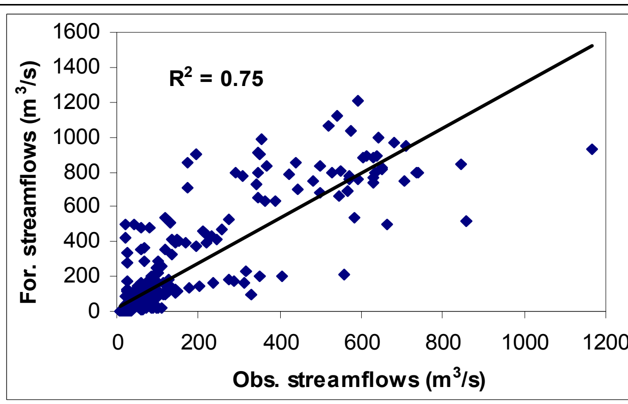

c) E-43: Before model calibration

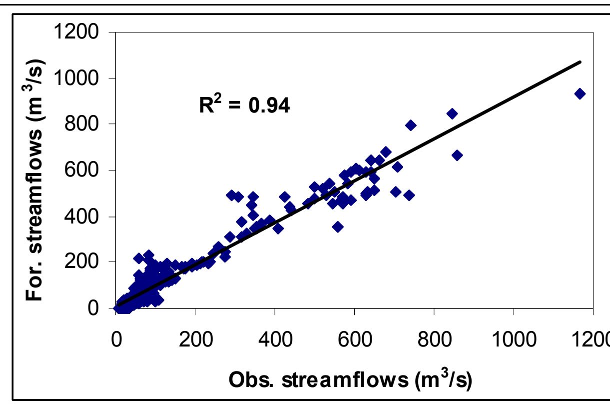

d) E-43: After model calibration

Figure 5.16: Regression between observed and forecasted streamflows at Ressano Garcia (a, b) and Magude (c, d) before and after model calibration

b) The Root-Mean-Square-Error (RMSE)

The RMSE for E-23 was equal to 3.9 m^3/s and for E-43 was 2.2 m^3/s. This means that in each maximal streamflow predicted by the model at E-23 there is an average error of 3.9 m^3/s and 2.2 m^3/s at E-43. Therefore the model is performing well if we consider that it has not included the contribution of discharge from Corumana dam at E-43 as well as the discharges from South African and Swaziland dams in the Incomati River at E-23.

5.3.4 Impact of Land Use Changes on Flow Regime

The impact of land use changes on streamflows was modelled for 6 of the sub-basins located in the upper, medium and lower part of the basin as shown in Figure 5.17, by comparing hydrographs generated under the land use scenarios of 1990 and 2010.These are the main sub-basins because they are the most developed in the basin. The rainfall figures used were for the period 2000 to 2004. In the coming subsection results for each sub-basin are presented.

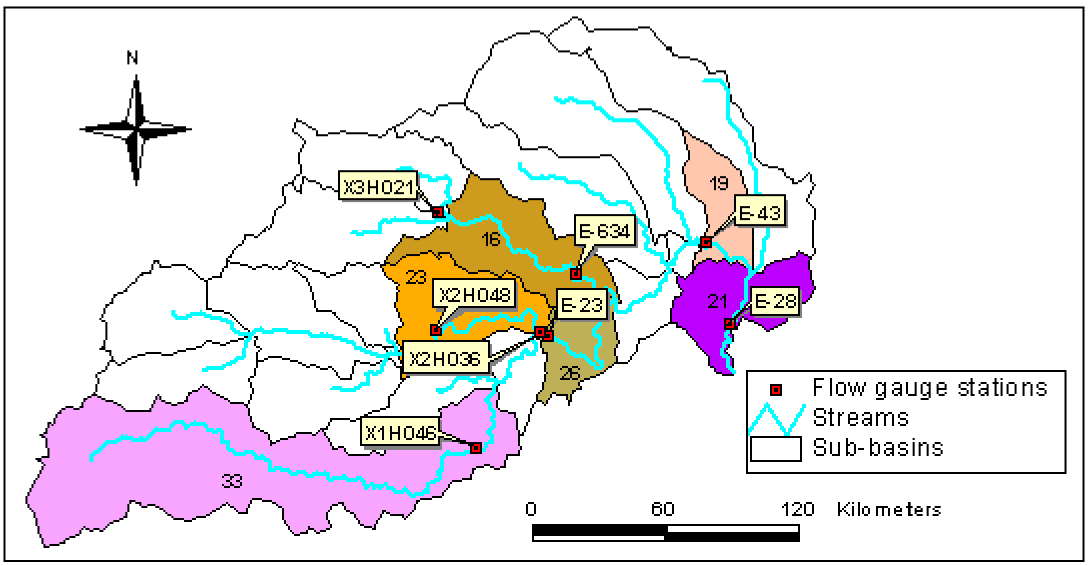

Figure 5.17: Spatial location of the analyzed sub-basins

a) Impact of Land Use Changes on Flow Regime in Sub-basin 16

Figure 5.18 presents the model outputs of simulations for 1990 and 2010 land use scenarios at sub-basin 16. The two hydrographs followed the same pattern for both high and low flows, and the hydrograph of the 2010 land use scenario produced the highest peak flow than the one for 1990 in the Julian day 2000044 (854.43 m^3/s). Both hydrographs peaked on the same days but in terms of recession time, the 2010 land use hydrograph was the quickest. For more than 95% of the time the two land use maps produced almost the same flow.

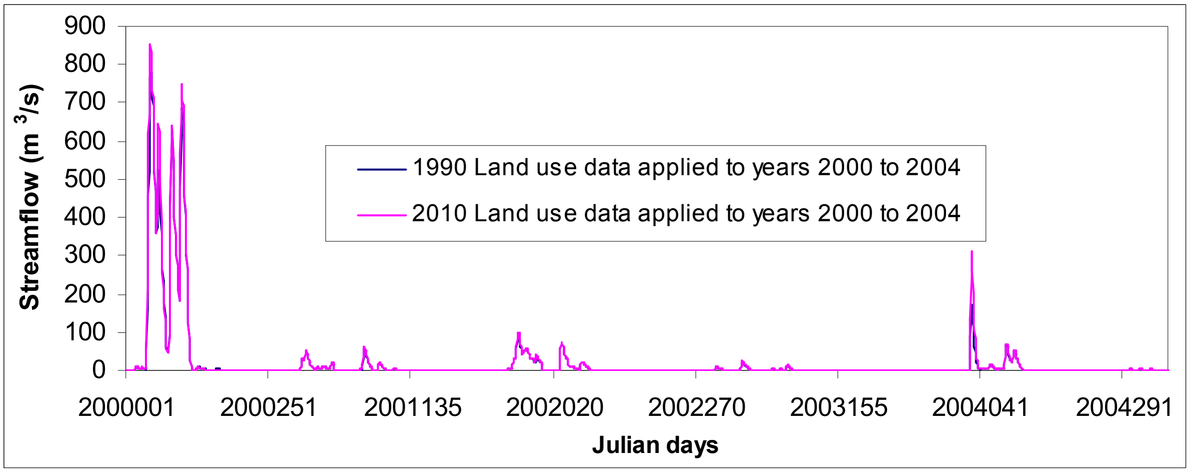

Figure 5.18: Simulation results for 1990 and 2010 land use maps for the sub-basin 16

The situation shown in Figure 5.18 suggests that for sub-basin 16, there were no significant changes in flow since 1990 to 2010. This sub-basin is part of the Sabie catchment which falls under the Kruger Park in South Africa which is a reserve park and is still in near pristine conditions. So the results shown by the Figure 5.20 are in agreement with the documented status of the catchment by TPTC (2010) and with the flow changes analysis results shown in the Section 5.2.2 of this thesis, that suggest a stable situation in terms of flows in the catchment since the 1980's.

b) Impact of Land Use Changes on Flow Regime in Sub-basin 21

This sub-basin is in the lower part of the Incomati basin and it receives all the flows from the basin before discharging into the sea. From Figure 5.19 it can be seen that in terms of hydrological response, the 2010 land use hydrograph was the fastest to generate runoff. In addition to that, the 2010 land use hydrograph produced the highest peak flow of about 4545.57 m^3/s on the Julian day 2000044. The second and third highest peak flows of 3123.75 m^3/s and 3129.31 m^3/s were produced by the 1990 land use hydrograph on the Julian days 2000081 and 2000099, respectively. In general, the 2010 land use hydrograph had the quickest recession time than the 1990 land use hydrograph. Regarding low flows, the two hydrographs followed the same trend but in general the 2010 land use hydrograph was slightly above the one for 1990.

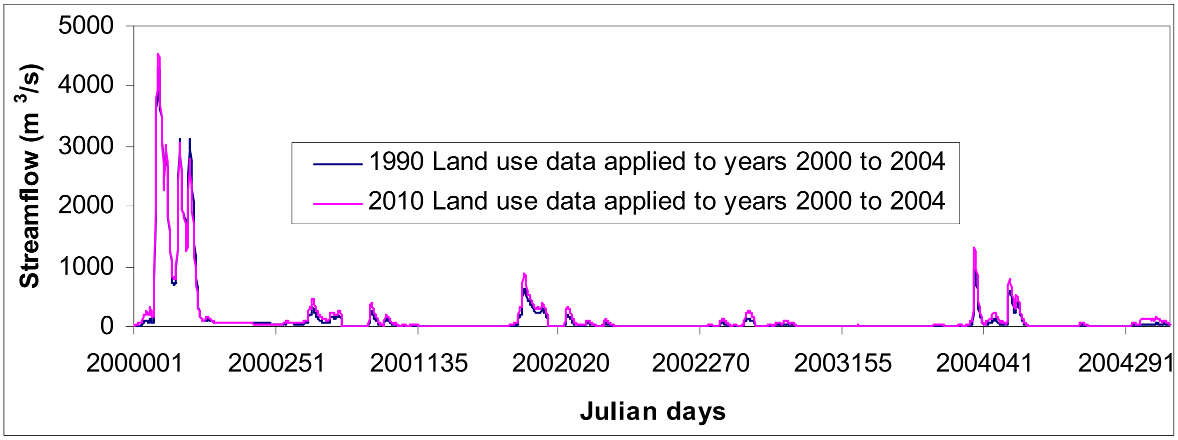

Figure 5.19: Simulation results for 1990 and 2010 land use maps for the sub-basin 21

The situation shown by Figure 5.19 suggests that the change in land use has resulted in an increase of the sub-basin response to rainfall events. This can be related to the urbanization that has taken place in this sub-basin as it covers the Manhiça and Marracuene districts which are amongst the most populated in the region according to the National Statistics Institute population census (2007). Another important factor to be considered in this sub-basin is the increase in commercial agriculture fields, where Xinavane and Maragra sugar cane plantations have increased their irrigated areas by more than 100% between 1990 and 2010 (TPTC, 2010). Furthermore, as suggested by Stipinovich (2005), increases in agricultural areas often result in a drop in interception rates, rapid delivery of storm flows to streams and reduction in infiltration capacity of the soils due to compaction.

c) Impact of Land Use Changes on Flow Regime in Sub-basin 23

This sub-basin lies under the Crocodile catchment in South Africa. The simulation outputs show a situation of similar response to rainfall events between the two land use hydrographs. The 1990 land use hydrograph produced the highest peak flows than the one of 2010 (1517.47 m^3/s and 678.07 m^3/s on Julian days 2000046 and 2000080, respectively). In general, both hydrographs peaked on the same days (Figure 5.20). For the two highest peaks registered, the 2010 land use hydrograph had the quickest recession time. For low flows (less than 200 m^3/s), which were observed for most of the time, the two hydrographs showed a similar response and produced flows of almost equal magnitude.

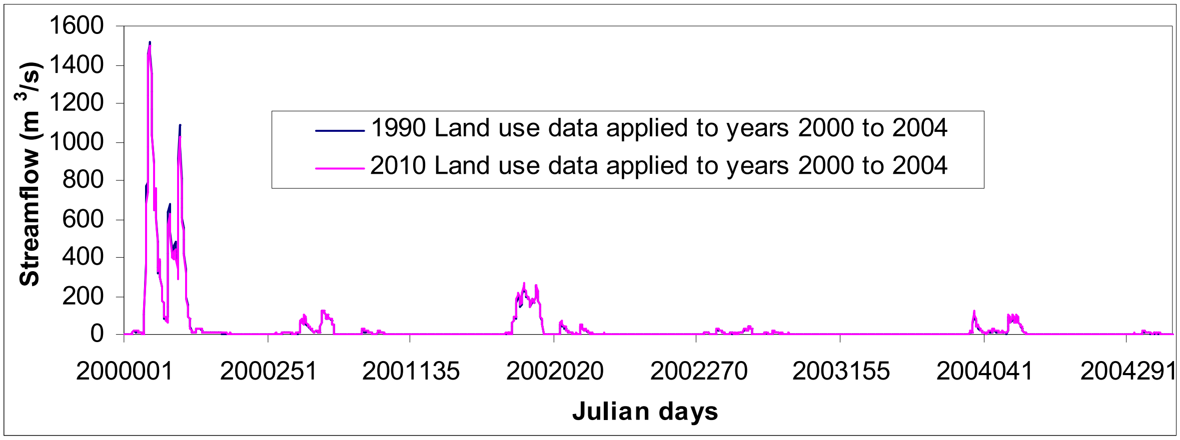

Figure 5.20: Simulation results for 1990 and 2010 land use maps for the sub-basin 23

Figure 5.20 indicates similarity on the flows produced by the 1990 and 2010 land use maps. This is in agreement with the flows analysis presented in the section 5.2.2 of this thesis, in which for the Crocodile catchment there has been a stable flow trend since 1960.

d) Impact of Land Use Changes on Flow Regime in Sub-basin 26

This sub-basin lies under the middle part of the basin on the Mozambican side as shown in Figure 5.17. The 2010 land use hydrograph showed the fastest response to initial rainfall events than the 1990 land use hydrograph and produced the highest peak flow (of about 2082.6 m^3/s). The 2010 land use hydrograph peaked 2 days before the 1990 land use hydrograph for the same amount of rainfall. In terms of recession time, the 2010 land use hydrograph was the quickest than that of 1990. For more than 95% of the time, the flow produced by the 2010 land use map was slightly above the one for 1990 (Figure 5.21).

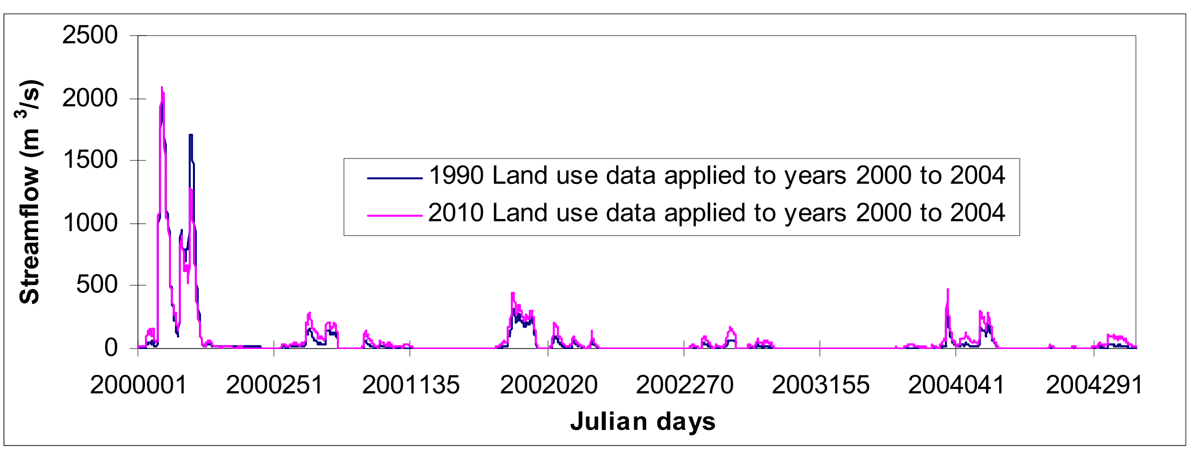

Figure 5.21: Simulation results for 1990 and 2010 land use maps for the sub-basin 26

The situation shown in Figure 5.21 suggests that land use changes resulted in generation of higher flows compared to 1990 land use map for the same climatic conditions. This can be attributed to an increase in settlements in the district of Moamba which is located in this sub-basin (National Statistics Institute, 2007).

e) Impact of Land Use Changes on Flow Regime in Sub-basin 19

At this sub-basin, the flow patterns produced by the 1990 and 2010 land use scenario were almost the same, however the 2010 land use hydrograph was the fastest in responding to rainfall events. According to Stipinovich (2005), this can be due to reduced infiltration in the compacted soils caused by increased mechanized agriculture. Intensive agriculture practised at Xinavane/Tongat Hullet sugar plantations could be major contributor to this situation.(Figure 5.22).

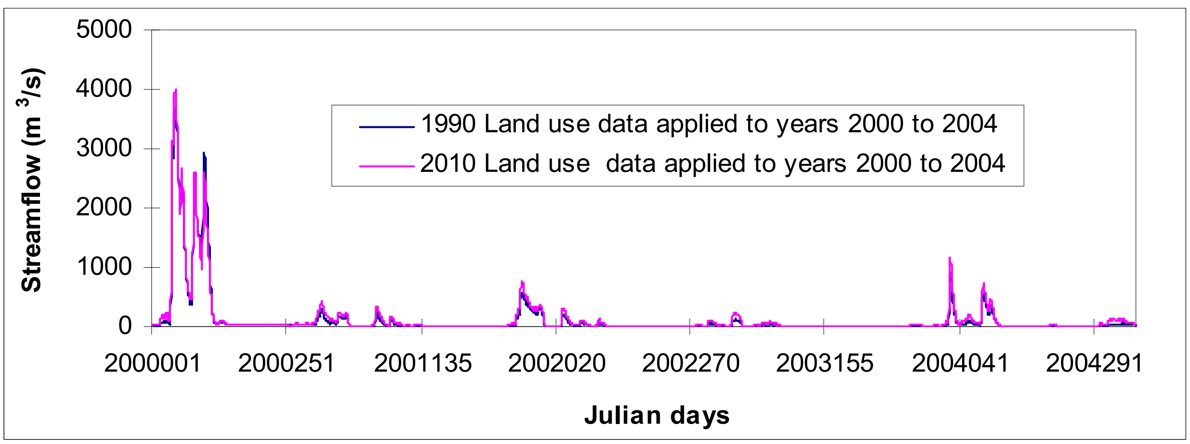

Figure 5.22: Simulation results for 1990 and 2010 land use maps for the sub-basin 19

f) Impact of Land Use Changes on Flow Regime in Sub-basin 33

This sub-basin is located in the Komati catchment and according to the model, the 1990 land use hydrograph produced the highest peak flow of about 704 m^3/s than the 2010 hydrograph (237.68 m^3/s) on Julian day 2000101. For both hydrographs, the date of peak was the same, but the time of recession was shorter for the 2010 land use hydrograph. Low flows (less than 150 m^3/s), for both hydrographs, followed a similar pattern but in general the 2010 land use hydrograph was above that of 1990 (Figure 5.23).

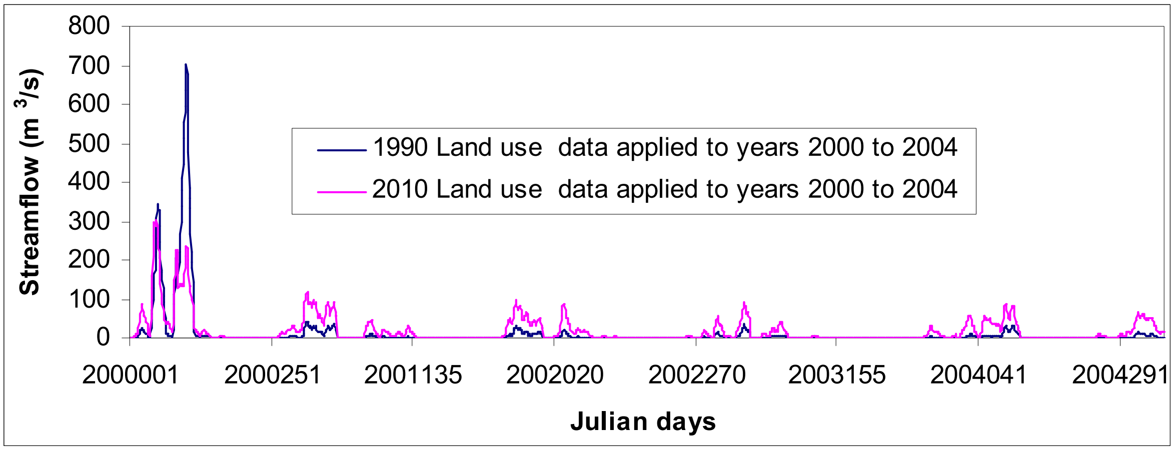

Figure 5.23: Simulation results for 1990 and 2010 land use maps for sub-basin 33

Figure 5.23 suggests that 1990 land use hydrograph showed better response in terms of flow generation than the 2010 land use hydrograph only for high rainfall events. On average, the 2010 land use map produced high flows than the 1990 land use map. This can be attributed to an increase in impervious surfaces in the sub-basin caused by the expansion of towns and increase in sugar cane plantation in Swaziland as documented by TPTC (2010). The situation could also be attributed to the construction of new dams like Maguga and other small agricultural dams in the same area. The dams have increased the impervious surface of the sub-basin altering the rate of portioning of the incoming rainfalls events.

5.3.5 Summary of Changes in Streamflows in the Main Sub-basins

Table 5.4 summarises the statistical analysis of the estimated changes of streamflows in the main sub-basins of the Incomati basin. The changes on streamflows due to land use changes were significant ($p<0.05$) in the sub-basins 26 and 33. For the other sub-basins the estimated streamflows changes were not statistically significant at $p<0.05$, meaning that the difference obtained was by chance.

Table 5.4: Statistical analysis of the changes in streamflows due to land use changes

Year	**Mean flow per Sub-basin (m^3/s)**					
	26	**21**	**19**	**23**	**33**	**16**
1990 Land use hydrograph	56.16	133.21	110.86	35.06	11.89	20.79
2010 Land use hydrograph	68.49	153.85	128.79	35.14	18.65	22.46
Change in flow (%)	**21.94**	**15.50**	**16.16**	**0.24**	**56.90**	**8.05**
Statistical significance (T –test, p<0.05)	**significant**	**Not significant**	**Not significant**	**Not significant**	**significant**	**Not significant**

The significant streamflow changes estimated for the sub-basins 26 and 33 suggest that the land use changes that have taken place have affected the hydrology of these sub-basins. Sub-basin 33 lies within the Komati catchment which is considered to be one of the catchments where major land use changes have taken place since 1991 (TPTC, 2010), mainly through conversion of forest and savannah areas to agricultural fields. These dynamics were stimulated by the construction of the Maguga dam in Swaziland. Sub-basin 26 lies within the Incomati catchment in Mozambique, where land use changes since the 1990 are visible, mainly through conversion of savannah and forest land to urban areas at Ressano Garcia village and Moamba District centre. In other sub-basins such as 16 and 23, where there have not been significant changes, the results obtained are in agreement with the flow change analysis presented in the section 5.2.2.

Mutie (2006) used the same model in the Mara River basin in Kenya and observed that land use hydrograph from year 2000, produced higher peak flows than the 1986 land use hydrograph Mutie (2006) also observed that the land use data from the year 2000 produced streamflows even at small rainfall magnitudes for which the 1973 data did not. So the results obtained in this work are similar to those reported by Mutie (2006) and Nkomo (2003) who modelled the water resources in the Komati catchment using the WAFLEX model and concluded that commercial afforestation created significant reduction of the natural runoff whilst deforestation increased the natural runoff.

5.4 Streamflows at Key Stations According to IIMA

According to IIMA (2002), the hydrometrical stations for flow control and the respective minimum flows to be maintained in the Incomati basin to sustain the ecology of the water course including the estuary are as presented in Table 5.5.

Table 5.5: Hydrometrical stations for flow control and minimum flows

River	Key Point	Interim Target Instream Flow	
		Mean (Mm^3/a)	Minimum (m^3/s)
Sabie	Lower Sabie	200	0.6
	Confluence with Incomati River	200	0.6
Crocodile	Tenbosh	245	1.2
Komati	Diepgezet	190	0.6
	Mananga	200	0.9
	Lebombo	42	1.0
Incomati	Ressano Garcia	290	2.6
	Sabie	290	2.6
	Marracuene	450	3.0

Due to data unavailability constraints, the analyses were performed for Lower Sabie, Tenbosh and Ressano Garcia.

5.4.1 Lower Sabie (X3H015)

The station is located in the Sabie catchment in South Africa. From Figure 5.24 it can be seen that the observed annual flows were below the IIMA stipulated ones only in 2002/2003. In terms of daily flows, the observed flows were above the minimum IIMA flows for 100% of the time from 2002/03 to 2009/10 (Figure 5.25). The annual rainfall figures in the same region followed a similar trend as the annual flows, where the maximum rainfall of 865 mm/a in 2005/06 generated a corresponding peak flow of 1000 Mm^3/a and the minimum rainfall of 327.5mm generated the minimum annual flow of 192 Mm^3/a. Although other factors could have influenced the flows, for this station the flows were a direct consequence of the observed rainfall.

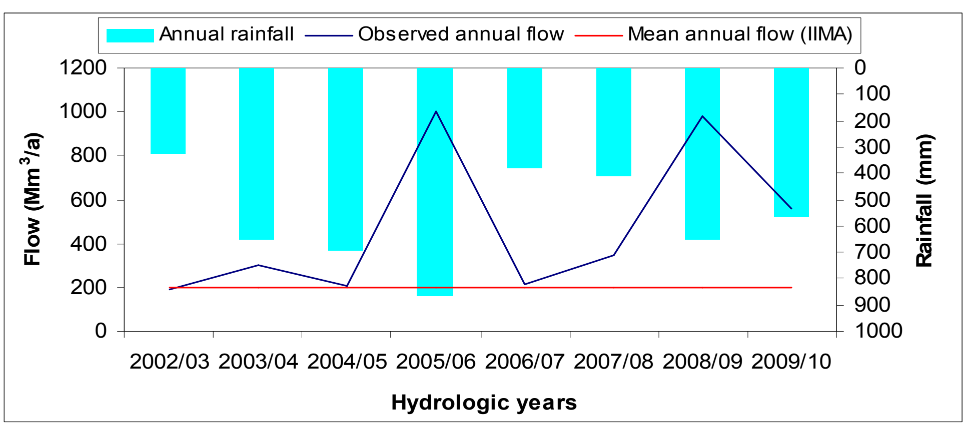

Figure 5.24: Comparison between observed annual flows and IIMA mean annual flows at Lower Sabie (X3H015)

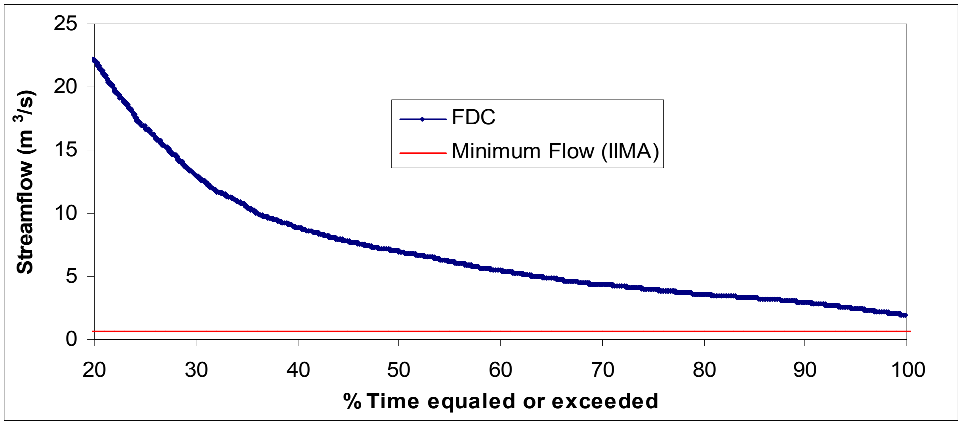

Figure 5.25: Level of compliance of daily IIMA minimum flows at Lower Sabie (X3H015)

5.4.2 Tenbosh (X2H016)

Tenbosh is located in the Crocodile River in South Africa and is one of the IIMA key stations for flow monitoring. From 2002/03 to 2009/10, the annual flows have not been in compliance with the stipulations three times, in 2002/03, 2004/05 and 2006/07 (Figure 5.26). The observed daily flows were below the IIMA minimum flows for 22% of the time between 2002/03 and 2009/10 (Figure 5.27). From the available rainfall data, it can be seen that there is a good level of agreement between flows and rainfall for the period before the year 2007/08. After 2007/08 the flows were not directly related to rainfall and this shows that there have been other factors influencing the flow pattern at Tenbosh. Therefore, rainfall can be considered as one of the driving factors for the non-compliance with the IIMA provisions although there is a need to acknowledge the effect of other factors.

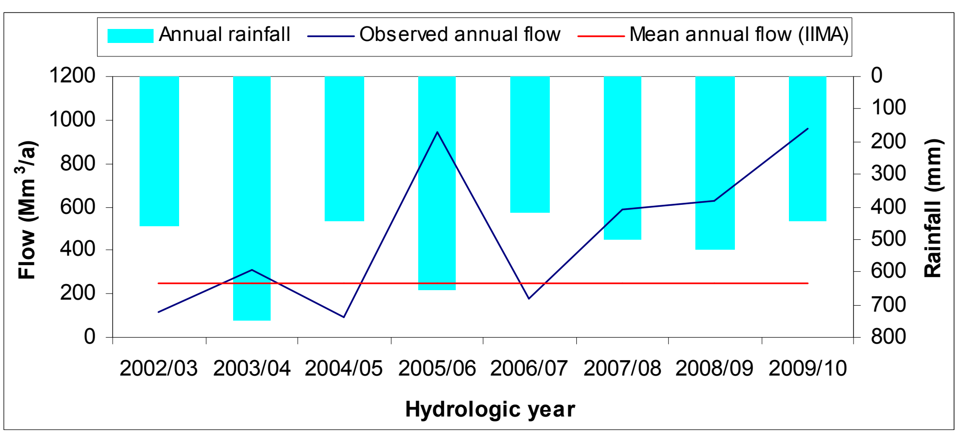

Figure 5.26: Comparison between observed annual flows and IIMA mean annual flows at Tenbosh (X2H016)

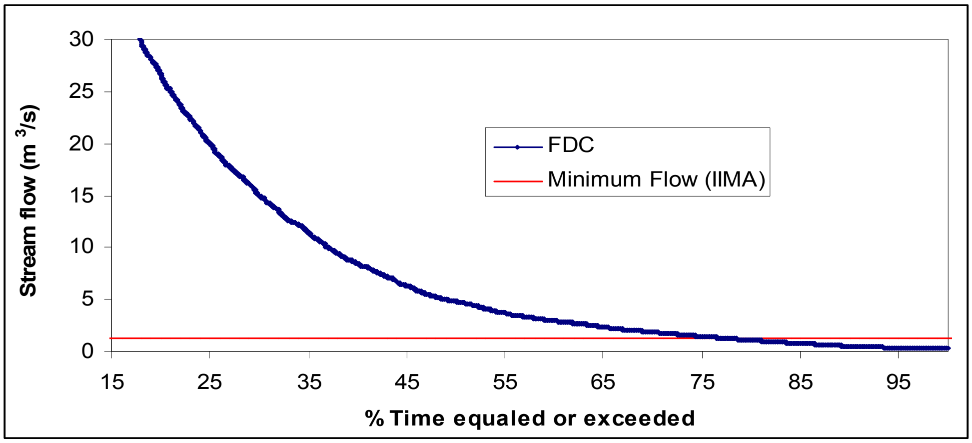

Figure 5.27: Level of compliance of daily IIMA minimum flows at Tenbosh (X2H016)

5.4.3 Ressano Garcia (E-23)

At Ressano Garcia, the annual observed flows were below the IIMA stipulations in the years 2002/03, 2004/05 and 2006/07. From the year, 2002/03 to 2007/08 the total observed rainfall in the same region followed the same trend, in which years of high and low observed annual flows coincided with high and low rainfall respectively (Figure 5.28). After 2007/08 the agreement between flows and rainfall was not observed and this shows that there have been other factors influencing the flows rather than rainfall. The results obtain from modelling suggest that land use change is one of the factor that have influenced the flow pattern at this station as it lies under sub-basin 26 considered as one the sub-basins in which significant streamflows changes have occurred as a result of land use change. The daily observed flows were below the IIMA minimum flows for 43% of the time since the agreement entered into enforcement in 2002 (Figure 5.29).

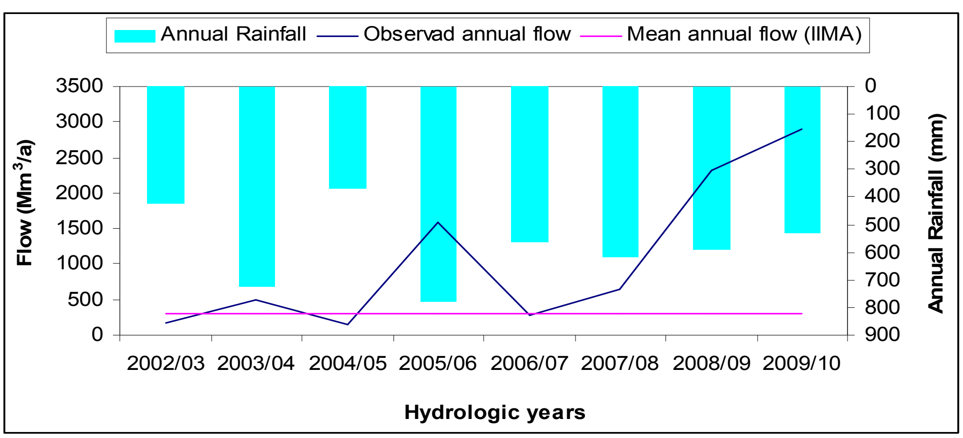

Figure 5.28: Comparison between observed annual flows and IIMA mean annual flows at Ressano Garcia (E-23)

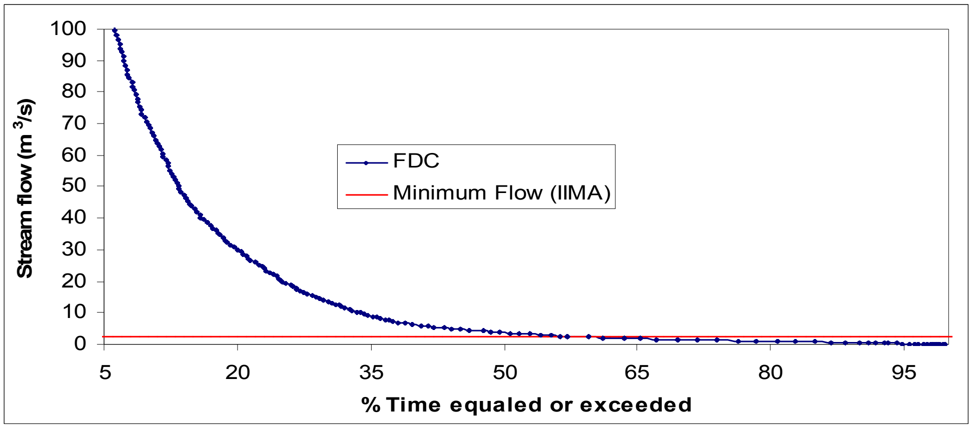

Figure 5.29: Level of compliance of daily IIMA minimum flows at Ressano Garcia (E-23)

5.5 Limitations on the Study Methods

The main limitation faced in this work was related to availability of reliable streamflow data mainly for the Swaziland part of the basin. The data was either not available or there was too much bureaucracy in obtaining it. This limited the performance of much detailed flow analysis in the basin.

The unavailability of Landsat images of good spectral quality and appropriate cloud cover for the same period or seasons of different years made it difficult to come up with better than the presented land use classification.

The time limitation was also of significance taking into account the amount of work involved in this Thesis. This limited the number of analyzed sub-basins.

CHAPTER 6

6.0 CONCLUSIONS AND RECOMMENDATIONS

6.1 Conclusions

From the study, the following conclusions were made:

1. Land use in the basin has been changing at a significant rate. Irrigated cropland, shrubland, urban and built-up land are the land use types with highest change (310%, 1056% and 285%, respectively).

2. There has been a change in the Incomati river inflows into Mozambique through the border station of Ressano Garcia (E-23). The average annual flow in the period between 1990/1991 and 2009/2010 was 52% below the average annual flow of the period between 1952/1953 and 1989/1990. In the Sabie River at E-634, there has not been a significant change in inflows to the Corumana dam in Mozambique.

3. The model indicates that there has been significant change ($p<0.05$) in streamflows due to land use changes in the sub-basins 26 and 33. These changes were in terms of peak flows, time to peak and the response to rainfall events. The 2010 land use produced hydrographs which responded faster to rainfall events than the 1990 land use. The peak flows generated by the 2010 land use hydrograph were of higher magnitude and faster time to peak than those of 1990. These results suggest that the reduction in streamflows at the border station of Ressano Garcia was related to other factors other than land use changes.

4. There have been some failures in some stations in complying with the provisions of the IIMA stipulated minimum flows to sustain the ecology including the estuary's ecosystems. These stations include Tenbosh (X2H016) and Ressano Garcia (E-23), with 22% and 43% of failure in complying with daily minimum flows since 2002/2003, respectively. However, the observed rainfall pattern in the stations region showed a pattern partially similar to the flows.

6.2 Recommendations

From the conclusions drawn, the following recommendations are made:

1. In medium to long term IWRM strategies in the basin must focus on regular investigation of the contribution of factors like agriculture to the flow regime as it has been changing at a high rate. This must be coordinated by the TPTC as the management board in charge.

2. In short term mechanisms of enforcing the IIMA stipulated flows in the basin need to be improved and monitored on the ground by the TPTC. This can be achieved through investments in near time data recorders (data loggers) and/ or through inclusion and implementation of the IIMA provisions in National day-to-day water management operations by the three countries.

3. In short term, automatic volumetric recording of agricultural water abstractions must be prioritised by the Water Management Entities of the three countries sharing the basin (ARA-Sul in Mozambique, DWA of Swaziland and ICMA in South Africa). That could allow an accurate quantification of water abstraction for irrigation and it can be achieved through investment in water meters.

4. In short term data recording and data and cost sharing need to be improved in the basin, mainly from the Swaziland side, in order to improve the management of the system and facilitate research aimed at improving the understanding of the basin. The TPTC needs to improve the coordination of the whole process of data sharing between the three countries.

6.3 Areas of Further Research

- Further research must be carried out in the same basin to account, in detail, for the contribution of other factors such as climate, water transfers, dam construction and operation to streamflow changes. This will complement the results of the present study and improve the understanding of land and water interactions in the basin.

REFERENCES

Alam, Z.R., Rahman, M. M. and Islam A. S. (2011) *Assessment of Climate Change Impact on the Meghna River Basin using Geomorphologically Based Hydrological Model (GBHM)*, 3rd International Conference on Water & Flood Management (ICWFM-2011).

Altman, D.G. (1991) *Practical Statistics for Medical Research*, Chapman & Hall, London, p285-288.

Ambroise, B., Beven, K. and Freer, J., (1996) Toward a Generalization of the TOPMODEL Concepts: Topographic indices of hydrological similarity, *Water Resources Research*, **Vol. 32** (7), p2135-2145.

Anderson, J.R, Hardy, E. E, Roach, J. T. and Witmer, R.E (1976) *A Land Use and Land Cover Classification System for Use with Remote Sensor Data,* Washington, United States of America.

Armitage, P.D. and Petts, G.E. (1992) *Biotic Score and Prediction to Assess the Effects of Water Abstractions on River Macroinvertebrates for Conservation Purposes*. Aquatic Conservation: Marine and Freshwater Ecosystems 2: p1-17.

Artan, G., Asante, K. and Kiesler, J. (2001) *Use and Description of Famine Early Warning System Flood Model, USGS*, Eros Data Centre, Sioux Falls, SD, 57198.

Asante, K.O., Artan A. G., Pervez S., Bandaragoda, C. and Verdin, J. P. (2008) *Technical Manual for the Geospatial Stream Flow Model (GeoSFM)*, U.S. Geological Survey, Reston, Virginia, USA.

Beven, K. (Ed.), (1997b) *Distributed Modelling in Hydrology: Applications of the TOPMODEL Concepts*, Wiley, Chichester.

Blackwell Science Ltd (1999) *Journal of Clinical Nursing*, **Vol. 8**, p762-763, Research in brief 763.

Bosch, J.M. and Hewlett, J.A. (1982) A Review of Catchment Experiments to Determine the Effect of Vegetation Changes on Water Yield and Evapotranspiration, *Journal of Hydrology,* **Vol. 55** (1-4), p3–23.

Brown, L.R. and Moyle, P.B. (1997) *Invading Species in the Eel River: Successes, Failures and Relationships with Resident Species*, Environmental Biology of Fishes, California, **Vol. 49**, p271-291.

Calder, I.R. (1992) *Hydrologic Effects of Land-use Change*, ed. in Chief D.R. Maidment, Handbook of Hydrology, USA, p13.1–13.50.

Chairat S. and Delleur J.W. (1993) Effects of Topographic Index Distribution on Predicted Runoff Using GRASS, Water Resources Bulletin, American Water Resources Association 29(6): 1029–1034.

DeFries, R. and Eshleman, K. N. (2004) *Land-use Change and Hydrologic Processes: A Major Focus for the Future*, **Vol. 18** (11), p2183–2186, USA.

Department of Water Affairs and Forestry (2009) *Inkomati Water Availability Assessment Study: Hydrology of the Komati River*, South Africa.

Duan, Q., Gupta, V.K., and Sorooshian, S., (1992) Effective and Efficient Global Optimization for Conceptual Rainfall-Runoff Models, *Water Resources Research*, **Vol. 28**, p1015–1031.

Edwards, K.A. (1979) *The Water Balance of the Mbeya Experimental Catchments*. In: Hydrological Research in East Africa (ed. by J. R. Blackie, K. A. Edwards and R. T. Clarke), E. Afr. Agric. For. J. Special Issue 43, p231-247.

Entenman, D., (2005) *Geo-spatial Stream Flow Model (GeoSFM),* USA.

Food and Agriculture Organization (FAO) (1998), *Soil Map of the World*, UNESCO, Paris, vol. 1-10 (1:5M scale maps and accompanying texts).

Gao B. and Yang D. (2009) *Impacts of Climate Variation and Land-Use Change on River Discharge in the Upstream of the Miyun Reservoir,* IAHS Publ. no. 335, p64-71, Tsinghua University, Beijing, China.

Government of the Republic of Mozambique (2003) *National Water Resources Development Plan for the Incomati River Basin,* NDF 197-5, Final Report, Maputo, Mozambique.

Guleid, A.; Verdin, J. and Asante, K., (2004) *Wide-Area Flood Risk Monitoring Model,* USGS, USA.

Gumindoga, W. (2010) *Hydrologic Impacts of Landuse Change in the Upper Gilgel Abay River Basin, Ethiopia: TOPMODEL Application,* MSc. Thesis Work, ITC, Enschede, The Netherlands.

Hsia, Y.J. and Koh, C.C. (1983) *Water Yield Resulting from Clear Cutting a Small Hardwood Basin in Central Taiwan,* In: Hydrology of Humid Tropical Regions with Particular Reference to the Hydrological Effects of Agriculture and Forestry Practice (ed. by R. Keller) (Proc. Hamburg Symp., August 1983), p215-220, IAHS Publ. no. 140.

Jenson S.K. and Domingue J.O., (1988) *Software Tools to Extract Topographic Structure from Digital Elevation Data for Geographic Information System Analysis: Photogrammetric Engineering and Remote Sensing*, **Vol. 54** (11), p1593-1600.

JIBS (2001) *Joint Incomati Basin Study Report Phase 2,* Consultec Report No: C14-99MRF/BKS ACRES Report No: P8491/08, Maputo/ Johannesburg.

Jones J.A, Grant G.E. (1996) Peak Flow Responses to Clear-Cutting and Roads in Small and Large Basins, Western Cascades, Oregon, *Water Resources Research* **Vol. 32** (4), p959–974.

LeMarie M., van der Zaag P., Mounting E.B. and Scholanus D. (2006) The Use of Remote Sensing for Monitoring Environmental Indicators: the Case of the Incomati Estuary, Mozambique, *Physics and Chemistry of the Earth,* **Vol. 31** (15-16), p857-863.

Lorup, J.K. and Hensen E. (1997) *Effect of Land Use on the Streamflow in the Southwestern Highlands of Tanzania*, Department of Hydrodynamics and Water Resources, Technical University of Denmark, Building 115, 2800 Lyngby, Denmark, IAHS Publ. no. 240.

Loveland, T.R., Reed, B.C., Brown, J.F., Ohlen, D.O., Zhu, J., Yang, L., and Merchant, J.W., (2000) Development of a Global Land Cover Characteristics Database and IGBP DISCover from 1-km AVHRR Data, *International Journal of Remote Sensing*, Vol. 21 (6), p1303–1330.

Mumeka, A. (1986) Effect of Deforestation and Subsistence Agriculture on Runoff of the Kafue River Headwaters, Zambia, *Hydrologic Science Journal*, **Vol. 31**, p543-554.

Mutie S.M, Mati B., Home P., Gadain H. And Gathenya J. (2006) *Evaluating Land Use Change Effects on River Flow Using USGS Geospatial Stream Flow Model in Mara River Basin*, Kenya.

Mutua, B.M and Klik, A. (2007) Predicting Daily Streamflow in Ungauged Rural Catchments: The Case of Masinga Catchment, Kenya, *Hydrologic Science Journal,* **Vol. 52** (2), p292-304.

National Directorate of Waters, NDW (1991) *Monograph of the Incomati River Basin,* **Vol. 1**, Mozambique.

National Statistics Institute (2007) *3rd General Population and Habitation Census,* http://www.ine.gov.mz/censo2007 , accessed on 16th May 2011.

Nijmeijer, R., (2001) *ILWIS 3.0 User's Guide*, International Institute for Geo-Information Science and Earth Observation-ITC, Enschede, The Netherlands.

Nkomo, S.M. (2003) *Water Resources Modelling in the Komati Catchment Shared by South Africa and Swaziland*, MSc thesis, University of Zimbabwe, Harare, Zimbabwe.

Nkomo, S. and van der Zaag P. (2004) *Equitable Water Allocation in a Heavily Committed International Catchment Area: The Case of the Komati Catchment*, In: Proceedings 4th WaterNet/WARFSA Symposium: Water, Science, Technology & Policy: Convergence and Action by All, Gaborone, 15–17 October.

Refsgaard, J.C. and Storm, B., (1995) *MIKE SHE, in Computer Models of Watershed Hydrology,* Vijay P. Singh, ed., Water Resources Publications, Highlands Ranch, Colorado, USA.

Reinhart K.G, Eschner A.R, Trimble Jr G.R. (1963) *Effect on Streamflow of Four Forest Practices in the Mountains of West Virginia*, US Forest Service Research Paper NE-1, Northeastern Forest Experiment Station, Upper Darby, PA.

Salas, J.D., (1993) *Analysis and modelling of hydrologic time series*, In: D.R. Maidment (Editor), Handbook of hydrology, McGraw-Hill, Inc, Texas, p19.1-19.72.

Schulze, R.E, (2000) *Modelling Hydrological Responses to Land Use and Climatic Change: The Southern African Perspective,* Ambio, **Vol. 29** (1), p13 – 22.

Sengo, D.J. (2003) *Effects of Water Management in Incomati River Basin into Estuarine System: A Downstream Perspective of Socio-economic Demands from the Estuarine Services*, MSc Thesis, UNESCO-IHE, Delft, The Netherlands.

Sengo, D.J., Kachapila, A., van der Zaag, P., Mul, M. and Nkomo, S. (2005) Valuing Environmental Water Pulses into the Incomati Estuary: Key to Achieving Equitable and Sustainable Utilisation of Transboundary Waters, *Physics and Chemistry of the Earth*, **Vol. 30** (11-16), p648–657.

Sherbinin A. (2002) *CIESIN Thematic Guide to Land-Use and Land-Cover Change (LUCC),* Center for International Earth Science Information Network (CIESIN), Columbia University, Palisades, NY, USA.

Smith, R.E. and Scott, D. F. (1992) *The Effects of Afforestation on Low Flows in Various Regions of South Africa,* Water SA, **Vol. 18** (3), p185-194.

Stipinovich, A. (2005) *Change in Land Cover and Water Abstraction: Modelling Runoff Effects in the Bot River Catchment,* MSc thesis, University of Stellensbosch, South Africa.

TIA. (2002) *Tripartite Interim Agreement between Mozambique, South Africa and Swaziland for Cooperation on the Protection and Sustainable Utilization of the Water Resources of the Incomati and Maputo Watercourses*, Johannesburg.

Tripartite Permanent Technical Committee (TPTC) between, Moçambique, South Africa, Swaziland (2010) *IAAP 3: Consultancy Services for Integrated Water Resources Management, Baseline Evaluation and Scoping Report PART C: STATUS QUO OF THE INCOMATI BASIN,* Report No.:IAAP 3: 03C – 2010.

United States Geological Survey–USGS (2008) *Technical Manual for the Geospatial Stream Flow Model (GeoSFM),* Reston, Virginia, USA.

United States of Geological Survey, (2006) Africa Data Dissemination Services http://igskmncnwb015.usgs.gov/adds/ visited 30th January 2011.

United States Geological Survey-USGS (2001) *HYDRO 1K data set for Africa*; *http://edcdaac.usgs.gov/glcc/glcc.html*, accessed on 6th January 2011.

Van der Zaag, P. (2008) *What Role of the Public for Achieving Peace and Prosperity in Heavily Committed Transboundary River Basins? Exploring Lessons from Southern Africa, with Particular Reference to the Incomati Basin*, UNESCO-IHE Institute for Water Education, ppt presentation.

Vaz, A.C. and van der Zaag, P. (2003) *Sharing the Incomati Waters: Cooperation and Competition in the Balance*. IHP Technical Documents in Hydrology—PCCP series No. 14. UNESCO, Paris, 102 pp.

Vilanculos A.C.F. (2006) *Towards Improving Flood Forecasting and Early Warning Systems Through Integrated Technology in The Limpopo Basin,* MSc thesis, University of Zimbabwe, Harare, Zimbabwe.

Walford, N., (1994) *Geographical Data Analysis*, UK.

Whitehead P.G, Robinson M. (1993) Experimental Basin Studies—an International and Historical Perspective of Forest Impacts, *Journal of Hydrology,* **Vol. 145** (3-4), p217–230.

Wood, P.J., Armitage, P.D., Cannan, C.E. and Petts, G.E. (1999) *Instream Mesohabitat Biodiversity in Three Groundwater Streams under Base-Flow Conditions,* Aquatic Conservation: Marine and Freshwater*,* **Vol. 9**, no. 3, p265-278.

Zahabiyoun, B. (1999) *Stochastic Generation of Daily Streamflow Data Incorporating Land Use And/ or Climate Change Effects*, Department of Civil Engineering, University of Newcastle upon Tyne, PhD Thesis, England, UK.

APPENDICES

APPENDIX A: SIGNIFICANCE OF SPEARMAN'S RANK CORRELATION

Work out the 'degrees of freedom' you need to use. This is the number of pairs in your sample minus 2 (n-2).

- Plot the Rsp result on the table.
- If it is below the line marked 5%, then it is possible your result was the product of chance and you must reject the hypothesis.
- If it is above the 0.1% significance level, then we can be 99.9% confident the correlation has not occurred by chance.
- If it is above 1%, but below 0.1%, you can say you are 99% confident.
- If it is above 5%, but below 1%, you can say you are 95% confident (i.e. statistically there is a 5% likelihood the result occurred by chance.

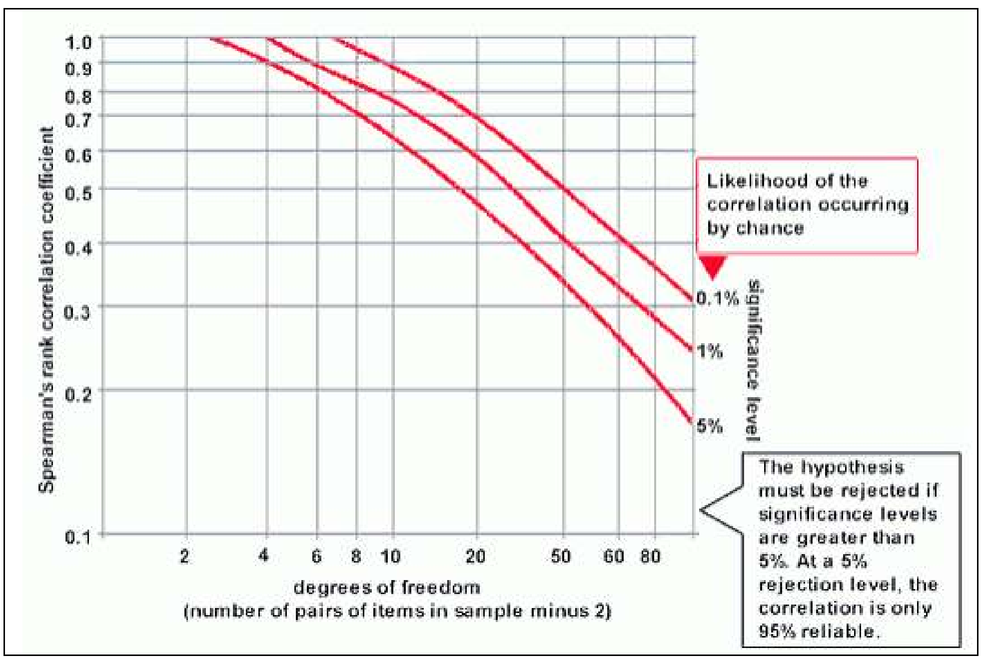

Figure A1: Spearman's significance level and level of freedom

APPENDIX B: LANDSAT IMAGES USED IN THE STUDY

Scene No.	Image Scene	Satellite Sensor	Mission	Data
1	P167R77	TM	5	27th July1990
2	P167R78	TM	5	27th July1990
3	P168R77	TM	5	25th June1990
4	P168R78	TM	5	25th June1990
5	P169R77	TM	5	12th June 1990
6	P169R78	TM	5	03rd June 1990
7	P167R77	TM	5	07th May 2000
8	P167R78	TM	5	07th May 2000
9	P168R77	TM	5	30th Aug 2000
10	P168R78	TM	5	30th May 2000
11	P169R77	TM	5	21st May 2000
12	P169R78	TM	5	21st May 2000
13	P167R77	TM	5	21st April 2004
14	P167R78	TM	5	21st April 2004
15	P168R77	TM	5	20th July 2004
16	P168R78	TM	5	20th July 2004
17	P169R77	TM	5	24th July 2004
18	P169R78	TM	5	24th July 2004
19	P167R77	TM	5	06th May 2010
20	P167R78	TM	5	19th May 2010
21	P168R77	TM	5	22nd May 2010
22	P168R78	TM	5	25th May 2010
23	P169R77	TM	5	06th May 2010
24	P169R78	TM	5	19th May 2010

APPENDIX C: DETAILS OF DATA QUALITY CHECKING

The sub-basins for which quality checking of satellite-derived rainfall and evapotranspiration data was done are as shown in Table C1. The term "normal" in the table refers to a situation whereby the data was observed as following the normal rainfall and evapotranspiration trend, in which the high values are observed from October to March and the low between April and September (Figures C1, C2, C3, C4 and C5).

Table C1: Sub-basins checked for quality of rainfall and evapotranspiration satellite-derived data

Sub basin of interest	**Contributing sub basins**	**Observed data pattern**				
		2000	2001	2002	2003	2004
26	17	normal	normal	normal	normal	normal
	22	normal	normal	normal	normal	normal
	23	normal	normal	normal	normal	normal
	24	normal	normal	normal	normal	normal
	25	normal	normal	normal	normal	normal
	26	normal	normal	normal	normal	normal
	27	normal	normal	normal	normal	normal
	28	normal	normal	normal	normal	normal
	30	normal	normal	normal	normal	normal
	31	normal	normal	normal	normal	normal
	33	normal	normal	normal	normal	normal
16	14	normal	normal	normal	normal	normal
	16	normal	normal	normal	normal	normal
	17	normal	normal	normal	normal	normal
15	10	normal	normal	normal	normal	normal
	15	normal	normal	normal	normal	normal
10	10	normal	normal	normal	normal	normal
19	10	normal	normal	normal	normal	normal
	15	normal	normal	normal	normal	normal
	16	normal	normal	normal	normal	normal
	18	normal	normal	normal	normal	normal
	19	normal	normal	normal	normal	normal
	20	normal	normal	normal	normal	normal
	26	normal	normal	normal	normal	normal

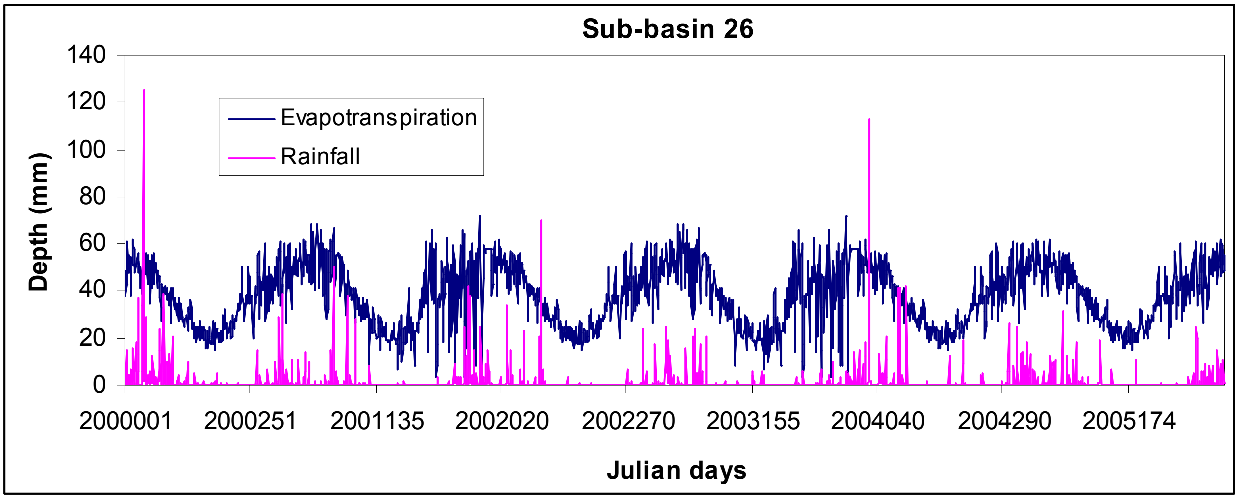

Figure C1: Pattern of the rainfall and evapotranspiration satellite-derived data in sub-basin 26

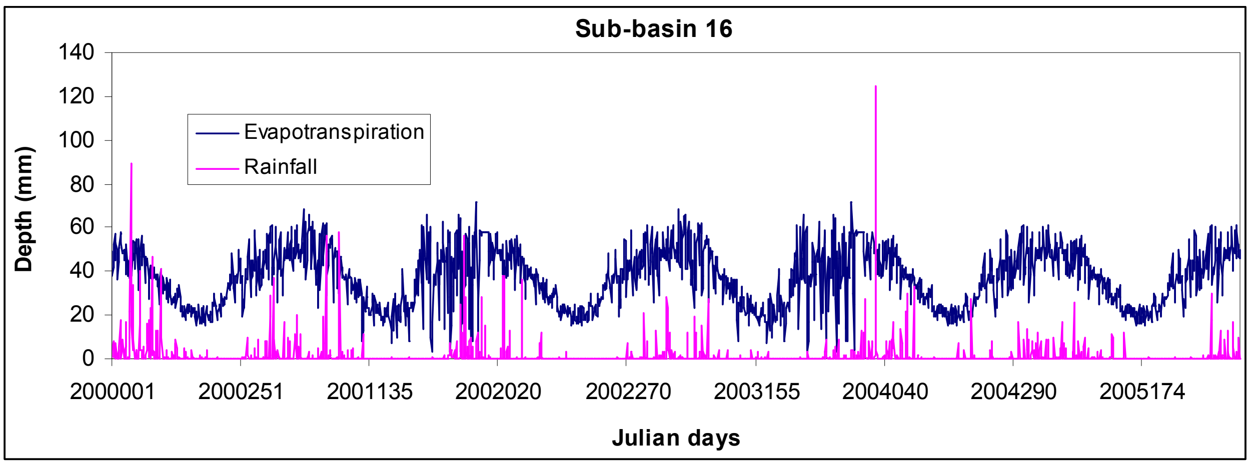

Figure C2: Pattern of the rainfall and evapotranspiration satellite-derived data in sub-basin 16

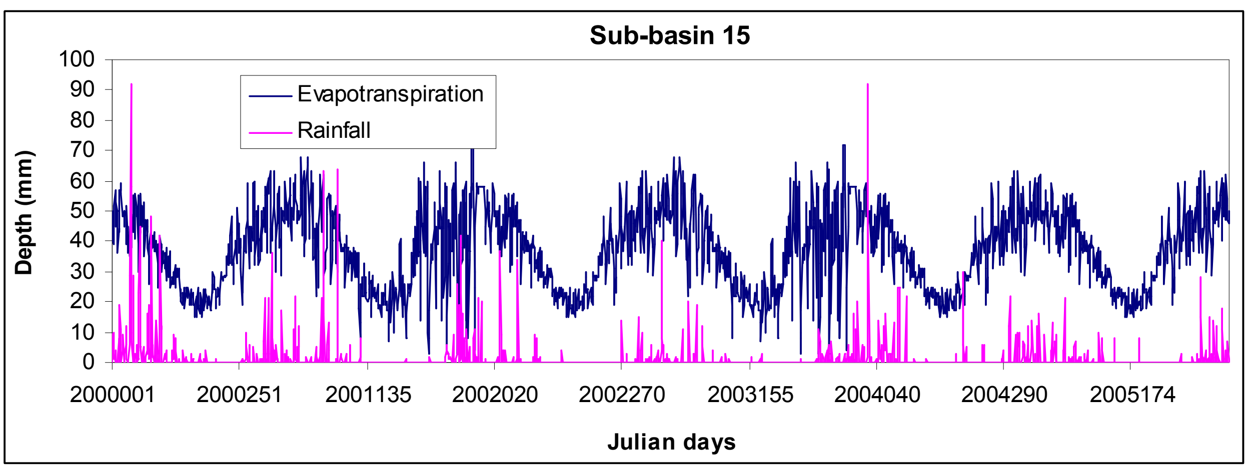

Figure C3: Pattern of the rainfall and evapotranspiration satellite-derived data in sub-basin 15

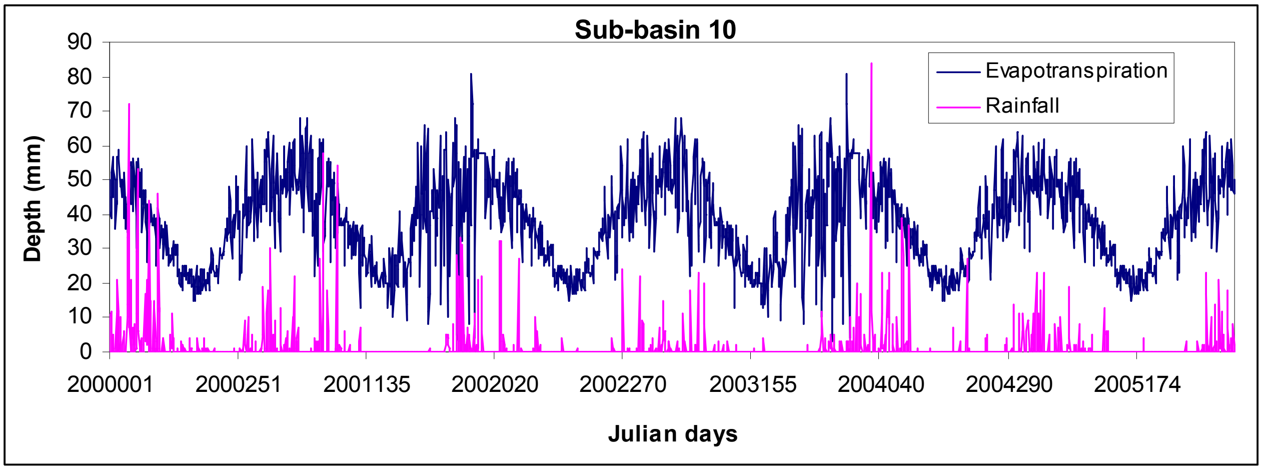

Figure C4: Pattern of the rainfall and evapotranspiration satellite-derived data in sub-basin 10

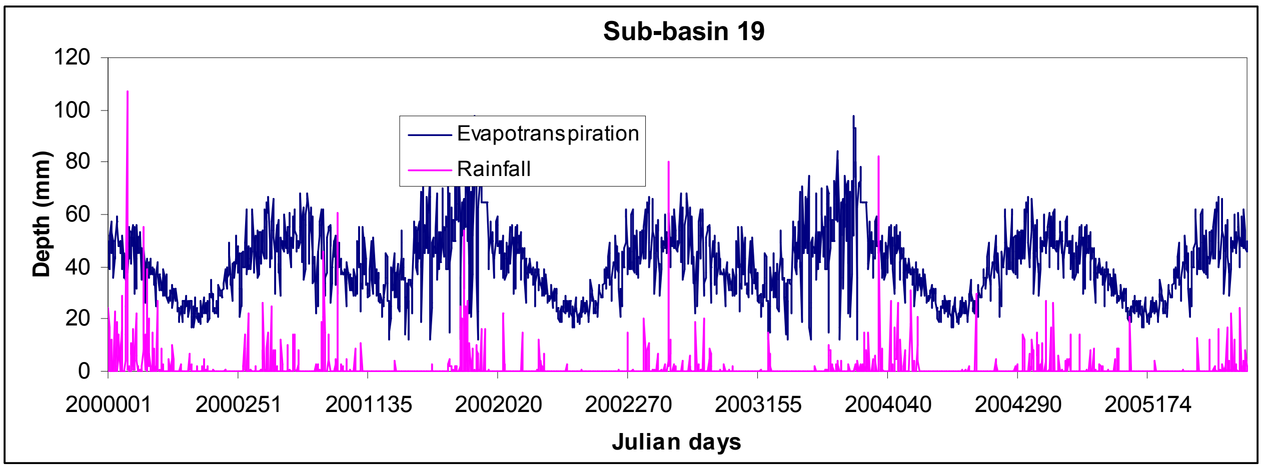

Figure C5: Pattern of the rainfall and evapotranspiration satellite-derived data in sub-basin 19